

Original Article	A Study of the Anatomical Variations in the number and Location of Palatine Foramina among Egyptian Population: A Dry Bone and Radiological Study <i>Hanan N. Gadallah, Mohamed E. El-Din Ibrahim, Ahmed S. Awad and Hadeer M. Ahmed Tohamy</i> <i>Department of Anatomy and Embryology, Radiology, Faculty of Medicine, Cairo University, Egypt,</i>
-------------------------	--

ABSTRACT

Background: The hard palate is an essential region of the skull; its gross anatomy and morphological variations have been of interest in many studies. The bones and dental structures of the palate are often preserved even in case of serious damage at or following death. The hard palate presents many important features including the greater and lesser palatine foramina. Locating the greater palatine foramen is of paramount importance for both dentists and oral and maxillofacial surgeons.

Aim of the work: The present work was designed to locate the greater palatine foramen (GPF) in relation to specific anatomical landmarks, assess the number of lesser palatine foramina and to estimate the direction of greater palatine canal in dry skulls and CT scans.

Material and Methods: The present study was carried out on 30 dry skulls (of un-identifiable gender) and 200 CT scans of brain and paranasal sinuses (100 adult males and 100 adult females). It was designed to demonstrate the number of lesser palatine foramina on each side, the presence of palatine crest, the direction of the greater palatine canal and the location of GPF in relation to specific surrounding anatomical landmarks being of paramount importance for both dentists, oral and maxillofacial surgeons.

Results: Variation in the location of GPF was remarkably common. Regarding linear measurements, no statistically significant difference existed between sides, but a statistically highly significant difference existed between males and females. Regarding the position of GPF in relation to maxillary molar teeth, the most frequent location was opposite the third maxillary molar (50% of dry skulls and 41% of CT scans). The direction of the greater palatine canal (GPC) was elucidated only in dry skulls; in individual specimens the direction on both sides was the same.

Conclusion: Regarding linear measurements, no statistically significant difference existed between sides, but a statistically highly significant difference existed between males and females.

Received: 22 November 2019, **Accepted:** 15 January 2020

Key Words: Dry skull, greater palatine foramen, radiological study.

Corresponding Author: Hanan N. Gadallah, Department of Anatomy and Embryology, Faculty of Medicine, Cairo University, Egypt. **Tel.:** 01223724723, **E-mail:** hanan.nabih2010@gmail.com

The Egyptian Journal of Anatomy, ISSN: 0013-2446, Vol. 43 No. 2

INTRODUCTION

The hard palate is an essential region of the skull; its gross anatomy and morphological variations have been of interest in many studies. The bones and dental structures of the palate are often preserved even in case of serious damage at or following death^[1].

The hard palate presents many important features including the greater and lesser palatine foramina. The lesser palatine foramina (LPF),

usually two, lie behind the greater palatine foramen (GPF) and pierce the pyramidal process of the palatine bone, which is wedged between the lower ends of the medial and lateral pterygoid plates. The LPF transmit the lesser palatine vessels as well as the middle and posterior palatine nerves. The palatine crest is a prominent bony ridge extending medially from behind the GPF^[3].

The GPF transmits the greater palatine nerve and vessels. The greater palatine nerve (GPN) emerges on the hard palate from the GPF and runs

forward in a groove up to the incisor teeth where it meets the terminal filaments of the nasopalatine nerves^[3]. The greater palatine artery (GPA) originates from the descending palatine branch of the maxillary artery in the pterygopalatine fossa (PPF), passes through the greater palatine canal (GPC) and emerges from the GPF on the palatal aspect of the third maxillary molar, to reach the hard palate^[4].

Locating the greater palatine foramen (GPF) is of paramount importance for dentists and oral and maxillofacial surgeons. However, publications in this field are lacking unanimity regarding the exact location of this foramen in relation to surrounding anatomical landmarks^[5].

The majority of textbooks locate GPF in a very general way, such as near the lateral or posterolateral palatal border or medial to or opposite the third maxillary molar^[6-8].

Anatomical studies on the placement of the GPF have been conducted in numerous populations, such as Thai^[9], Brazilian^[10], Korean^[11], Nigerian^[12], Egyptian^[1], and Turkish^[13].

Evidence supports a racial variation in the position of the GPF^[9,14,15]. Detailed knowledge of the population specific data on biometric features of the GPF is mandatory in therapeutic, local anesthetic and surgical manipulations in the maxillo-facial region^[16].

Furthermore, it is essential to determine the location of the GPF for palatal donor tissue and greater palatine nerve block anesthesia. Knowing the exact location of the GPF is important also for mobilization of the greater palatine artery in closure of oroantral fistula using mucoperiosteal pedicled palatal flaps^[13].

Although many authors have studied the location of GPF, literature is lacking in studies relevant to Egyptians apart from that of Shalaby^[1] which was conducted on dry skulls only.

MATERIAL AND METHODS

1) Material:

A. Dry bone study: Thirty adult human skulls obtained from the Anatomy Department, Faculty

of Medicine, Cairo University were included in this study.

. Inclusion criteria: adult human skulls (> 25 years old).

. Exclusion criteria: presence of pathological changes in the region of maxilla, including developmental and traumatic changes.

B. Radiological study:

CT scans of skulls for examination of brain or paranasal sinuses of 200 adult persons, 100 males and 100 females were included in this study. The radiographs were obtained from a private radiology center.

. Inclusion criteria: CT scans of skulls for examination of brain or paranasal sinuses of adult persons of both sexes.

. Exclusion criteria: radiographs showing pathological changes in the region of maxilla (including developmental and traumatic changes).

2) Methods

A. Dry bone study:

Morphological Parameters:

□ **The following parameters were investigated:**

1. Number of lesser palatine foramina (LPF) on each side (Fig. 1A)

2. Presence of palatine crest on each side (Fig. 1A)

3. Location of the GPF in relation to maxillary molar teeth: either opposite the second maxillary molar (M2), between M2-M3, opposite M3 or behind M3^[14].

4. Direction of greater palatine canal (GPC) by inserting a needle into the GPF. The orientation of the GPC was described as anteromedial, anterior or anterolateral^[9].

Morphometric Parameters:**□ Measurements were taken from the center of GPF to:**

1. Posterior border of hard palate [PBHP] (shortest distance) (Fig. 1B)
2. Midline maxillary suture [MMS] (shortest perpendicular distance)(Fig. 2A)
3. Posterior nasal spine [PNS](Fig. 2B)
4. Center of incisive fossa [IF](Fig. 3A)
5. Center of opposite GPF (Fig. 3B) □.

□ All measurements were taken using a double tipped compass, transferred on a ruler and interpreted in millimeters.

□ All measurements were done thrice and the mean was recorded to decrease the bias errors.

□ The center of the GPF as well as the incisive fossa were established after inserting a piece of playdough (Fig. 1A).

B) Radiological study:

□ An e-film DICOM viewer version 2, a program for radiograph analysis and measurement, was applied to estimate morphological parameters and to calculate the linear measurements.

□ All data were obtained from CT scans axial view.

Morphological parameters:

1. Number of lesser palatine foramina (LPF) on each side (Fig. 4A)
2. Presence of palatine crest on each side (Fig. 4A)
3. Location of the GPF in relation to maxillary molar teeth (Fig. 5)

□ The location of GPF was described as either opposite the second maxillary molar (M2), between M2-M3, opposite M3 or behind M3.

□ The location of GPF was determined by drawing tangents parallel to the middle and distal aspects of the second and third maxillary molars which demonstrate an overlap with the GPF in the new depth of axial reconstruction^[22].

□ In the present study, this method was modified as follows:

a. The screen was divided on the e-film viewer into two parts (A and B).

b. The same axial cuts were retrieved in both parts.

c. A transverse line passing through the center of GPF in image B was drawn.

d. Another line parallel to the first one was drawn in image A.

e. A new depth of axial reconstruction demonstrated an overlap between the previous two lines, thus locating the GPF in relation to maxillary molar teeth.

Morphometric parameters:**□ The dimensions of the GPF (Fig. 4B) were estimated as follows:**

a. The longest anteroposterior (AP) and lateral-medial (LM) dimensions were measured.

b. The center of GPF was set at the point of intersection of the longest AP and LM dimensions.

c. The shape (or form) of GPF was determined by dividing AP by LM dimensions:

- Values equal one, indicates a circular foramen
- Values greater than one, indicates an AP elongated foramen
- Values less than one, indicates a LM elongated foramen^[15].

□ Measurements on CT scans were performed from the center of GPF to:

1. Posterior border of hard palate (shortest distance) (Fig. 6A)

2. Midline maxillary suture (shortest perpendicular distance) (Fig. 6B)
3. Posterior nasal spine (Fig. 7A)
4. Center of incisive fossa (Fig. 7B)
5. Center of opposite GPF (Fig. 8)

C) Statistical study:

Statistical analysis was performed using statistical package for social sciences (SPSS) version 21.0 (IBM corporation, Somers, NY, USA) statistical software. The frequency of

nominal data was done. The association among the different nominal variables regarding side and gender was explored using Chi square (X²) tests.

The quantitative data were expressed as means ± standard deviation (SD). The data were examined by Kolmogorov Smirnov test for normality. Independent t test was performed to compare between the different variables regarding side and gender.

The results were considered significant at $p\text{-value} \leq 0.05$ and highly significant at $p\text{-value} \leq 0.01$.

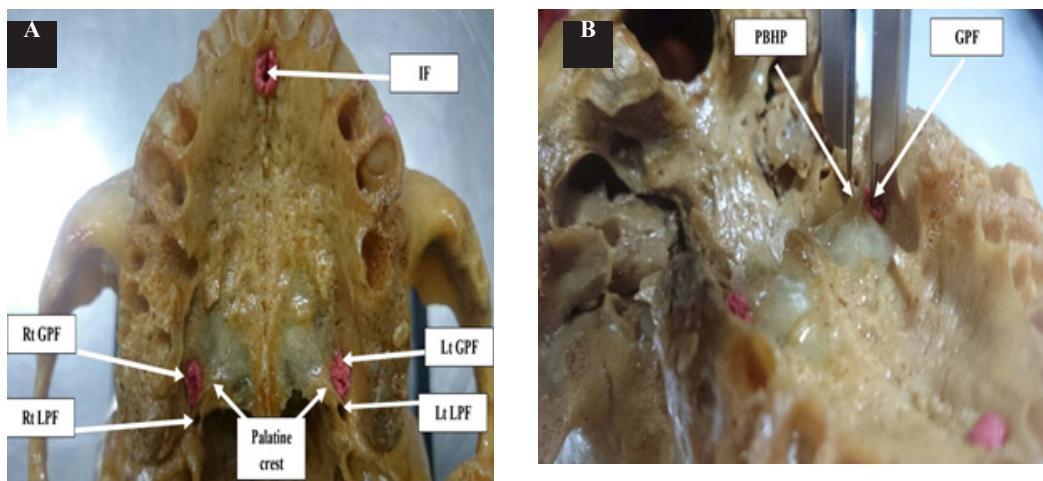


Fig. 1: A photograph of the hard palate illustrating, A. How the center of greater palatine foramen (GPF) as well as the center of incisive fossa (IF) are established after inserting pieces of playdough. The lesser palatine foramina (LPF) are also identified, B. The shortest distance from the center of greater palatine foramen (GPF) to posterior border of hard palate (PBHP).

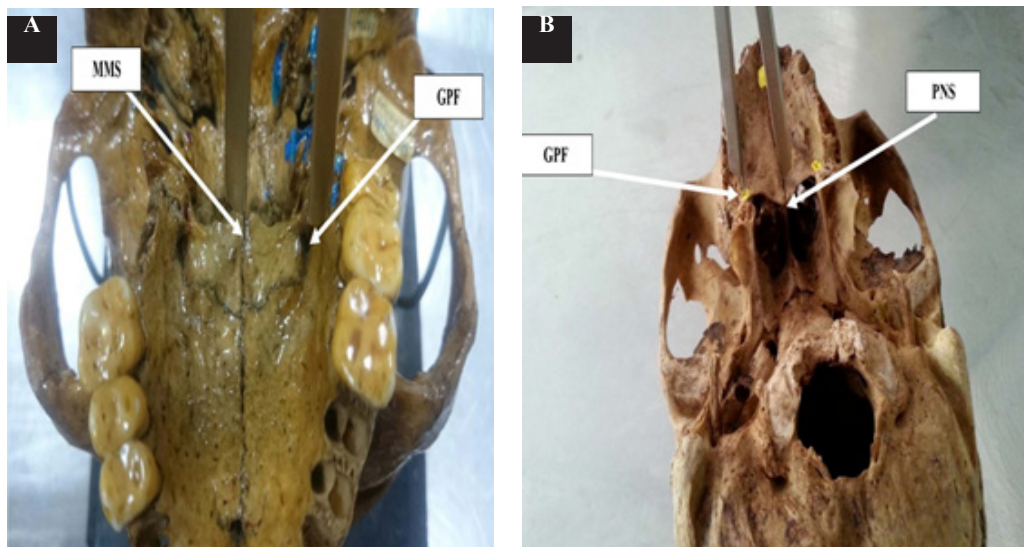


Fig. 2: A photograph of the hard palate (HP) illustrating, A. The shortest perpendicular distance from the center of greater palatine foramen (GPF) to midline maxillary suture (MMS), B. The distance from the center of greater palatine foramen (GPF) to posterior nasal spine (PNS).

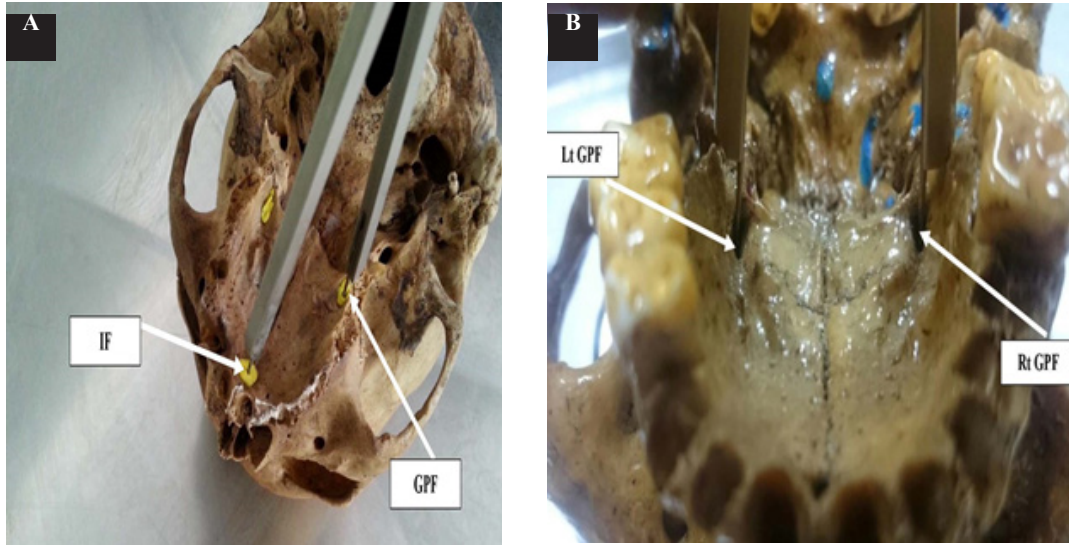


Fig. 3: A photograph of the hard palate illustrating, A. The distance from the center of greater palatine foramen (GPF) to center of incisive fossa (IF), B. The distance from the center of greater palatine foramen (GPF) to the center of opposite GPF

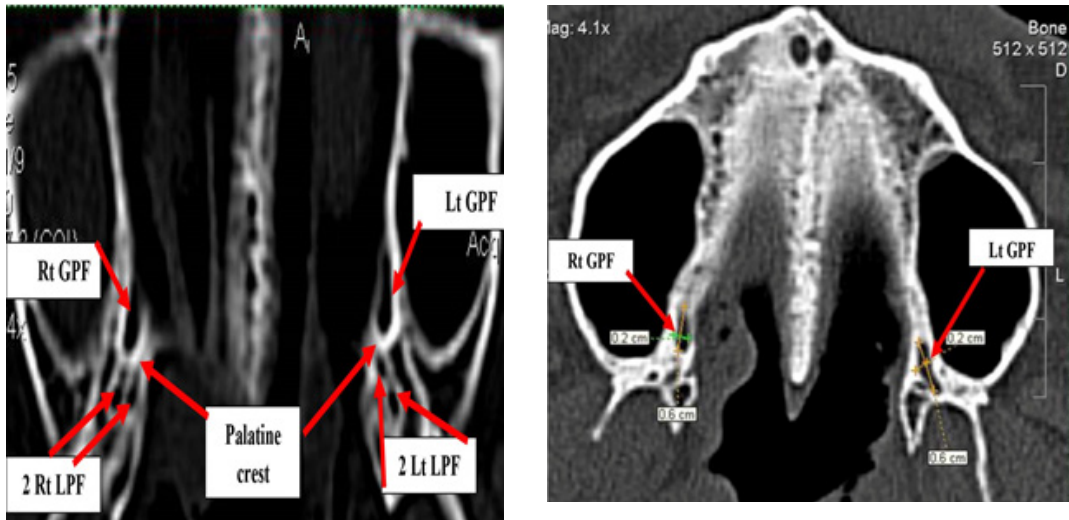


Fig. 4: A. A brain CT scan B. Paranasal sinuses CT scan of a male patient at the region of hard palate, illustrating A. The number of lesser palatine foramina (LPF) as well the presence of palatine crest and greater palatine foramen (GPF) on both sides. B. The dimensions of the greater palatine foramen (GPF)

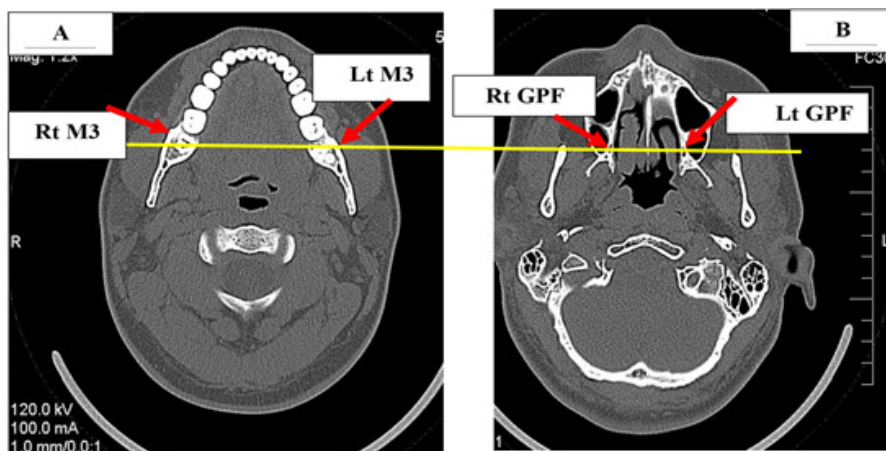


Fig. 5: Paranasal sinuses CT scan of a female patient at the region of hard palate, illustrating the location of right and left greater palatine foramina (GPF)(B) in relation to right and left third maxillary molars (M3)(A).

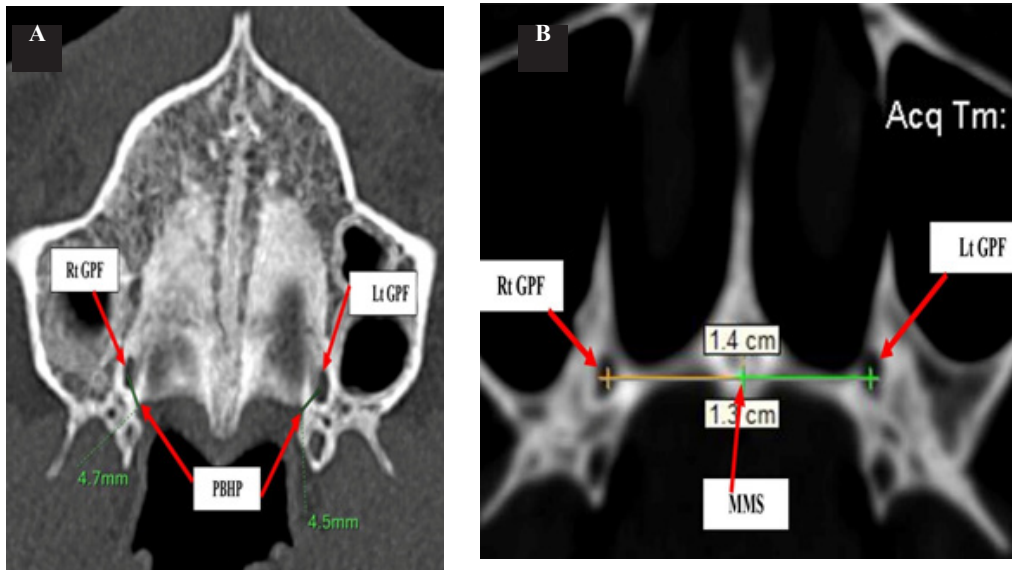


Fig. 6: A brain CT scan of a female patient at the hard palate, illustrating, A. The shortest distance from the center of greater palatine foramen (GPF) to posterior border of hard palate (PBHP). B. The shortest perpendicular distance from the center of greater palatine foramen(GPF) to midline maxillary suture (MMS)

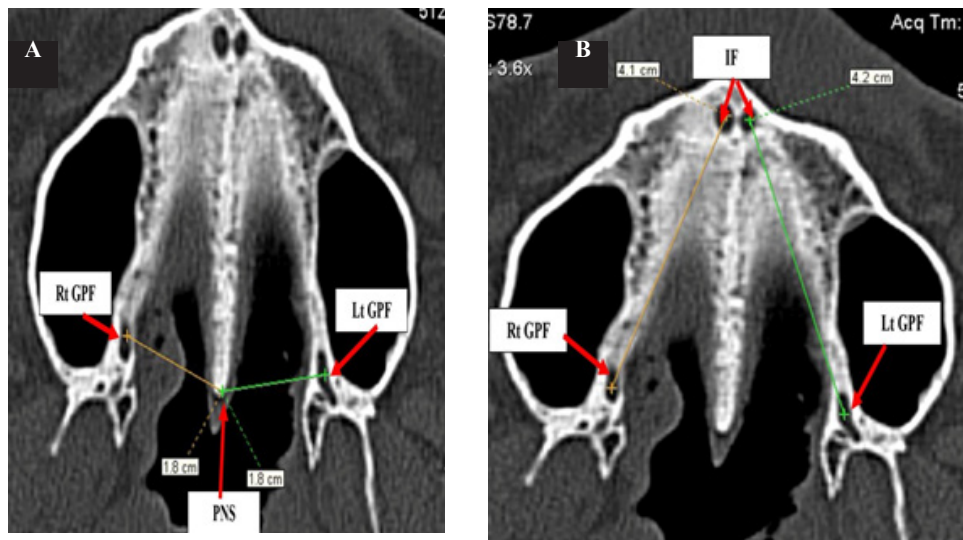


Fig. 7: Paranasal sinuses CT scan of a male patient at the hard palate, illustrating, A. The distance from the center of greater palatine foramen (GPF) to posterior nasal spine (PNS). B. The distance from the center of greater palatine foramen (GPF) to the center of incisive foramina (IF)

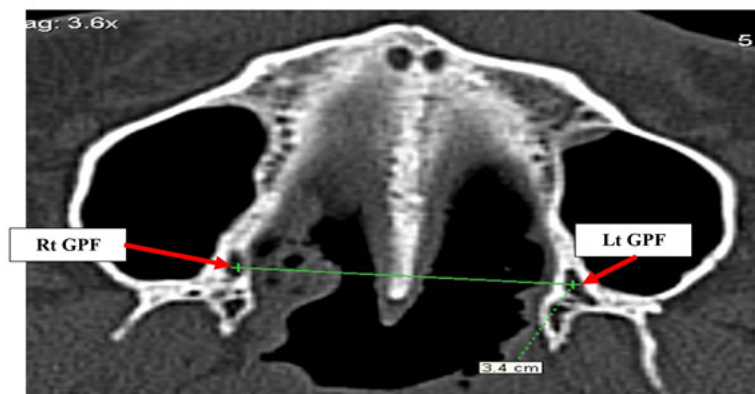


Fig. 8: Paranasal sinuses CT scan at the region of hard palate of the same patient in Fig. 7, illustrating the distance from the center of greater palatine foramen (GPF) to the center of opposite GPF

RESULTS

A) Dry bone study:

□ Morphological parameters:

1. Number of lesser palatine foramina (LPF):

The number of lesser palatine foramina was variable (Graph 1A). The presence of 2 lesser palatine foramina was most frequent (56.7%) (Fig.9). One lesser palatine foramen was detected in 26.7% (Figs.1A, 9A) and three foramina in 16.7% (Fig.10). Regarding the side, (Graph 1B) on the right side, two foramina were detected in 60% (Fig.9), one foramen in 26.7% (Fig.1A) and three foramina in 13.3% (Fig.10B). On the left side, two foramina were observed in 53.3% (Fig. 9B), one foramen in 26.7% (Fig.9A) and three foramina in 20% (Fig.10). All data are represented in (Table 1).

2. Presence of palatine crest:

The presence of palatine crest was a constant finding in all examined skulls (Figs.1A, 9).

3. Location of GPF in relation to maxillary molar teeth:

The GPF was located opposite M3 in 50% (Figs. 10A, 11A), could not be decided in 30% (Figs. 9, 10B), between M2-M3 in 13.3% (Fig. 11B) and opposite M2 in 6.7% (Fig. 12B). In every individual skull, the location of the GPF (Graph 2) was the same on both sides (Figs. 10A, 11, 12A). All data are represented in (Table 2).

4. The direction of greater palatine canal (GPC):

The GPC (Graph 3) was anteromedial in 73% (Fig. 12B), anterior in 23.3% (Fig. 13A) and anterolateral in 3.3% (Fig. 13B). The direction of the canal was always the same on both sides (Figs.12B, 13). All data are represented in (Table 3).

□ Morphometric parameters:

On the right side, the GPF was positioned 5.74 ± 1.31 mm from PBHP, 16 ± 1.30 mm from MMS, 17.66 ± 1.40 mm from PNS and 39.7 ± 2.43 mm from IF. On the left side, it was positioned 5.61 ± 1.17 mm from PBHP, 16.13 ± 1.2 mm from MMS, 17.77 ± 1.54 mm from PNS and 39.98 ± 2.36 mm from IF (Figs. 1B, 2B,3A). All data are represented in (Table 4) and (Graph 4).

The distance from the center of the GPF to the center of the opposite GPF was $31.81 \pm .58$ mm (Fig. 3B).

B) Radiological study:

□ Morphological parameters:

1. Number of lesser palatine foramina (LPF):

□ In the CT scans, regarding the number (Graph 5A), the presence of one lesser palatine foramen (LPF) was most frequent (75.5%) (Figs. 14A, 15A). Two LPF were observed in 22% (Figs. 14A, 15B, 16B) and three foramina in 2% (Figs. 14B, 16A). Absent foramina was encountered in 0.5% (Fig. 16B). Regarding the side (Graph 5B), on the right side, one foramen existed in 76% (Figs. 14A, 15A), two foramina in 23% (Fig. 15B) and three in 1% (Fig. 16A). On the left side, one foramen existed in 75% (Fig. 15A), two foramina 21% (Figs. 14A, 15B), three in 3% (Figs. 14B, 16A) and absent foramina was met with in 1% (Fig. 16B). All data are represented in (Table 5).

□ Regarding the gender (Graph 5C), males showed absent LPF in 1% (Fig. 16B), one foramen in 76% (Fig. 15A) and two foramina in 23% (Fig. 15B). Females showed one LPF in 75% (Fig. 14A), two foramina in 21% (Fig. 14A) and three foramina in 4% (Figs. 14B, 16A). All data are represented in (Table 6).

2. Presence of palatine crest:

The presence of palatine crest has been a constant finding in all examined CT scans (Figs. 14, 15A).

3. Location of GPF in relation to maxillary molar teeth:

□ The GPF (Graph 6A) was most frequently located opposite M3 (41%) (Figs.17, 20). It was found behind M3 in 25.8% (Fig.18), between M2-M3 in 23.3% (Figs.19, 20) and opposite M2 in 10% (Fig. 21). Regarding the side (Graph 6B), on the right side, the GPF was located opposite M3 in 40% (Fig. 17), behind M3 in 26% (Fig. 18), between M2-M3 in 24% (Figs. 19, 20), and opposite M2 in 10% (Fig. 21). On the left side, it was located opposite M3 in 42% (Fig. 17), behind M3 in 25.5% (Fig. 18), between M2-M3 in 22.5% (Fig. 19) and opposite M2 in 16% (Fig. 21). All data are represented in (Table 7).

Regarding the location of GPF in relation to maxillary molars in both males and females, several locations were encountered, opposite M3 (Figs. 17, 20) in 47.5% of males and 34.5% of females, between M2-M3 (Figs. 19, 20) in 27% of males and 19.5% of females, behind M3 (Fig. 18) in 21.5% of males and 30% of females and opposite M2 (Fig. 21) in 4% of males and 16% of females. All data are represented in (Table 8) and (Graph 6C).

□ *Morphometric parameters:*

• *The dimensions of the greater palatine foramen (GPF):*

On the right side, the mean AP diameter of the GPF was 3.94 ± 1.13 mm and the LM diameter was 2.17 ± 0.59 mm (Fig.22). On the left side, the mean AP diameter was 4.22 ± 1.21 mm and the LM diameter was 2.28 ± 0.74 mm (Fig.22). All data are represented in (Table 9) and (Graph 7A).

In males, the mean AP diameter of the GPF was 4.39 ± 1.2 mm and the mean LM diameter was 2.47 ± 0.70 mm (Figs. 22A, 22D). In females, the mean AP diameter was 3.77 ± 1.07 mm and the mean LM diameter was 1.98 ± 0.53 mm (Figs. 22A, 22D). All data are represented in (Table 10) and (Graph 7B).

The GPF (Graph 8A) was AP elongated in 90.5% (Figs. 22A, 22B) and circular in 9.5% (Figs. 22C, 22D). Regarding the side (Graph 8B), on the right side, the GPF was AP elongated in 90% (Figs. 22A, 22B) and circular in 10%

(Figs. 22C, 22D). On the left side, it was AP elongated in 91% (Figs. 22A, 22B) and circular in 9% (Figs. 22C, 22D). All data are represented in (Table 11).

In males, the GPF was AP elongated in 94% (Fig. 22A) and circular in 6% (Fig. 22C). In females, it was AP elongated in 87% (Fig. 22B) and circular in 13% (Fig. 22D). All data are represented in (Table 12) and (Graph 8C).

• *Measurements from the center of GPF to surrounding anatomical landmarks:*

On the right side, the GPF was positioned 3.9 ± 1.21 mm from PBHP (Figs. 6A, 23A), 14.95 ± 1.3 mm from MMS (Figs. 6B, 23B), 16.55 ± 1.61 mm from PNS (Figs. 7A, 24A) and 38.06 ± 3.10 mm from IF (Figs. 7B, 24B). On the left side, the GPF was positioned 3.93 ± 1.13 mm from PBHP (Figs. 6A, 23A), 14.99 ± 1.24 mm from MMS (Figs. 6B, 23B), 16.48 ± 1.6 mm from PNS (Figs. 7A, 24A) and 37.96 ± 3.17 mm from IF (Figs. 7B, 24B). All data are represented in (Table 13) and (Graph 9A).

In males, the GPF was positioned 4.22 ± 1.21 mm from PBHP (Fig. 23A), 15.37 ± 1.21 mm from MMS (Fig. 23B), 17.13 ± 1.54 mm from PNS (Fig. 7A) and 38.89 ± 3.28 mm from IF (Fig. 7B). In females, the GPF was positioned 3.61 ± 1.04 mm from PBHP (Fig. 6A), 14.57 ± 1.21 mm from MMS (Fig. 6B), 15.9 ± 1.42 mm from PNS (Fig. 24A) and 37.13 ± 2.70 mm from IF (Fig. 24B). All data are represented in (Table 14) and (Graph 9B).

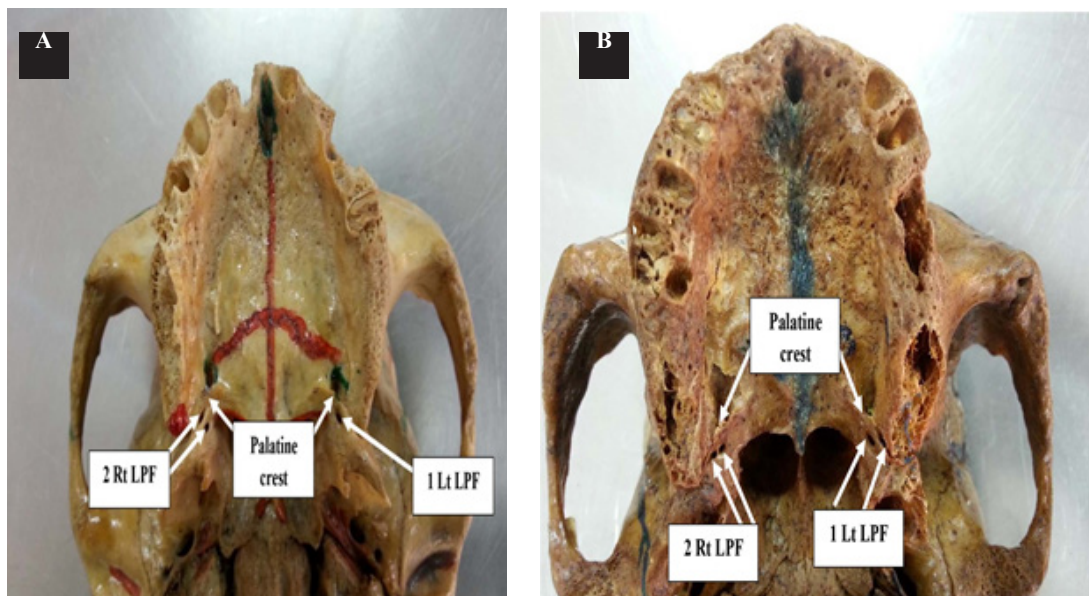


Fig. 9: A photograph of the hard palate illustrating, A. Single lesser palatine foramen (LPF) on the left side and two LPF on the right. B. Two lesser palatine foramina (LPF) on both sides.

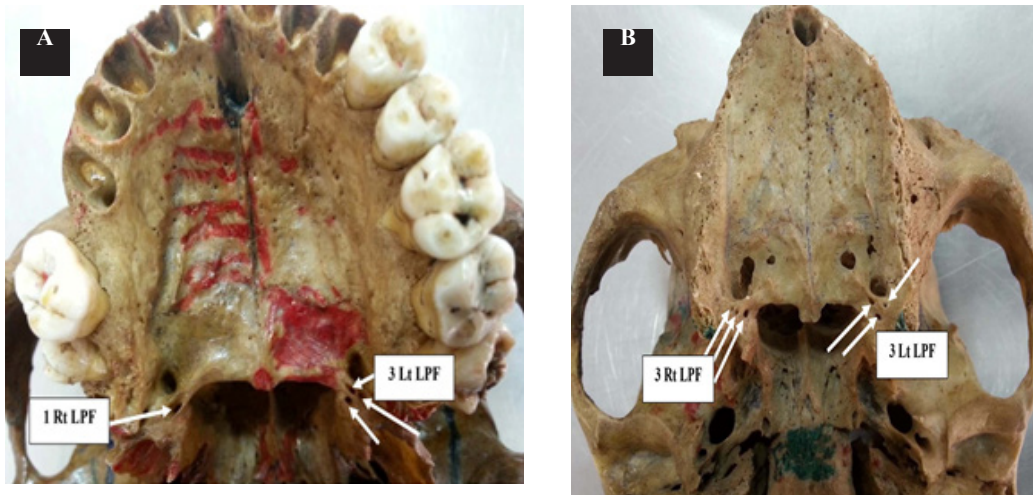


Fig. 10: A photograph of the hard palate illustrating, A. A single lesser palatine foramen (L.P.F) on the right side and three L.P.F on the left. B. Three lesser palatine foramina (L.P.F) on both sides.

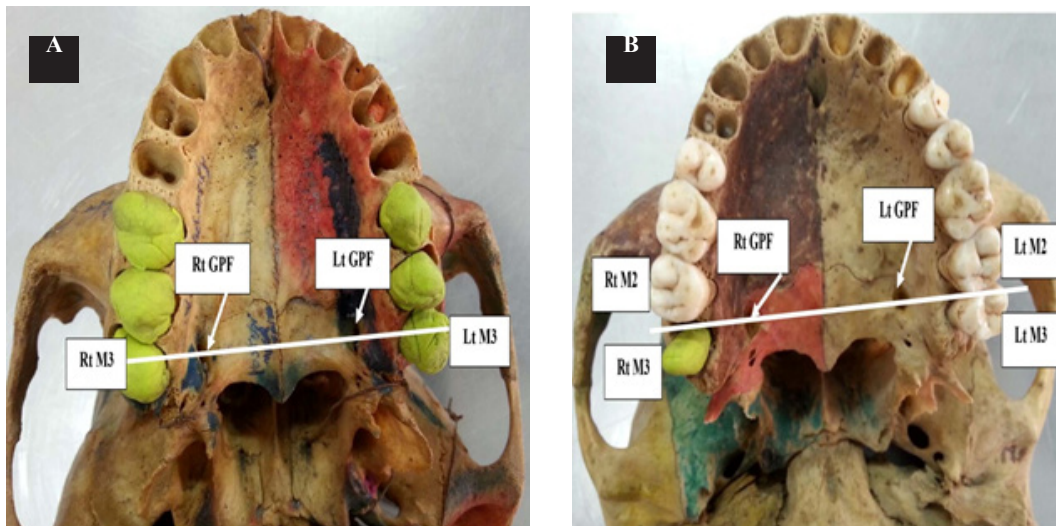


Fig. 11: A photograph of the hard palate illustrating the greater palatine foramen (GPF) located; A. Opposite the third maxillary molar (M3) on both sides, B. Between the second and third maxillary molars (M2- M3) on both sides.

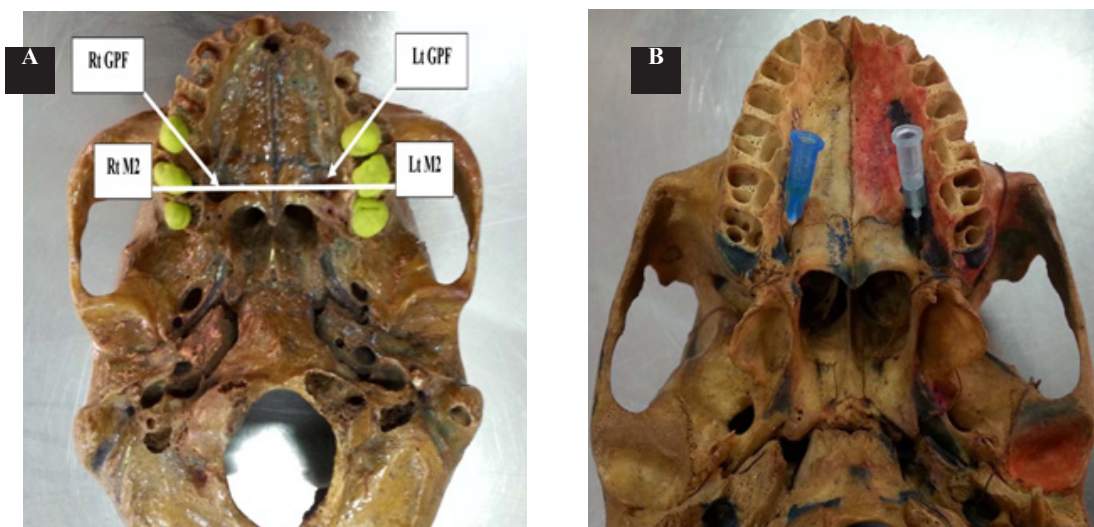


Fig. 12: A photograph of the hard palate illustrating, A. The greater palatine foramen (GPF) located opposite the second maxillary molar (M2) on both sides. B. Anteromedially directed needles inside greater palatine canal on both sides.

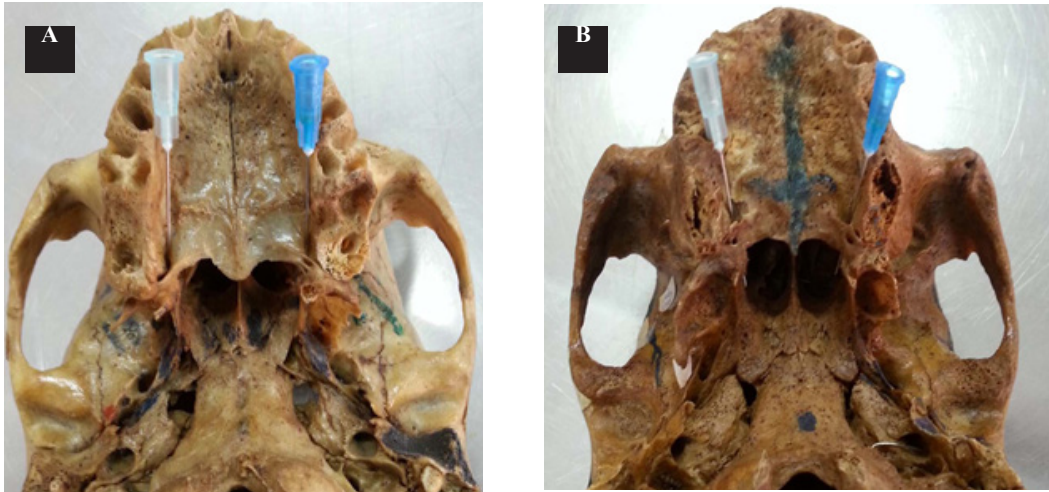


Fig. 13: A photograph of the hard palate illustrating, A. Anteriorly directed needles inside greater palatine canal on both sides. B. Anterolaterally directed needles inside greater palatine canal on both sides.

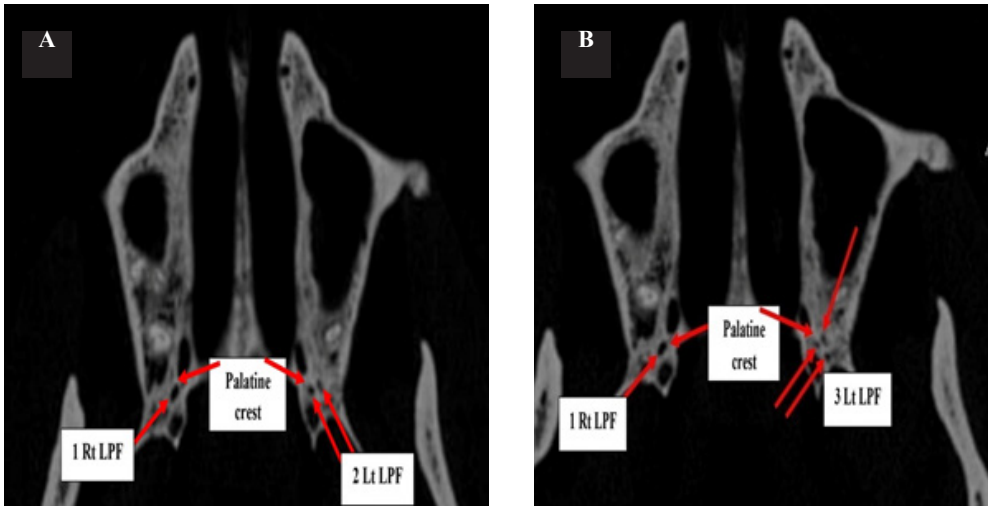


Fig. 14: Paranasal sinuses CT scan of a female patient at the region of hard palate, illustrating, A. A single lesser palatine foramen (LPF) on the right side and 2 LPF on the left. B. A single lesser palatine foramen (LPF) on the right side and three LPF on the left.



Fig. 15: A brain CT scan of a male patient at the region of hard palate, illustrating, A. A single lesser palatine foramen (LPF) on the both sides. B. Two lesser palatine foramina (LPF) on both sides.

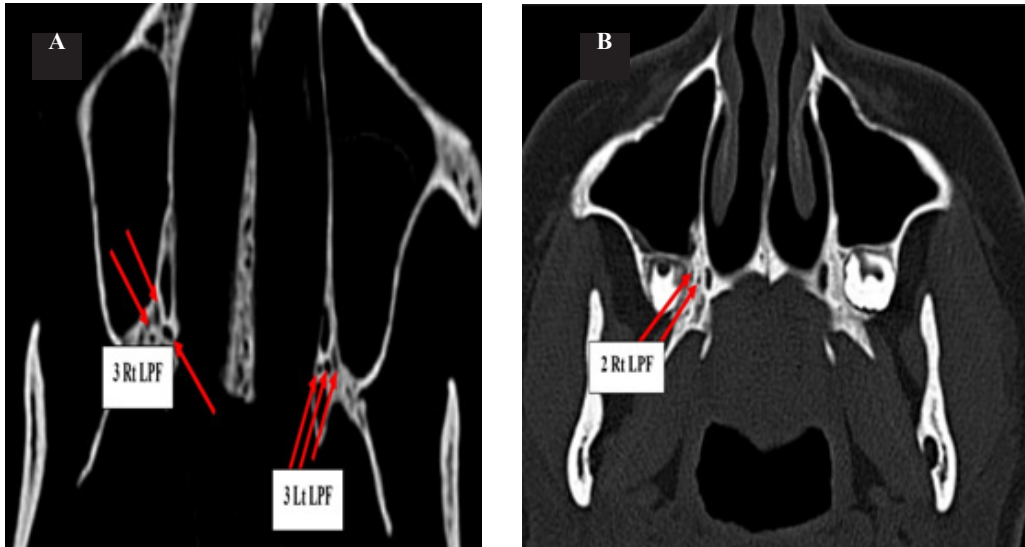


Fig. 16: A. A brain CT scan of a female patient skull at the region of hard palate, illustrating three lesser palatine foramina (LPF) on each side. B. Paranasal sinuses CT scan of a male patient at the region of hard palate, illustrating two lesser palatine foramina (LPF) on the right side and absent LPF on the left

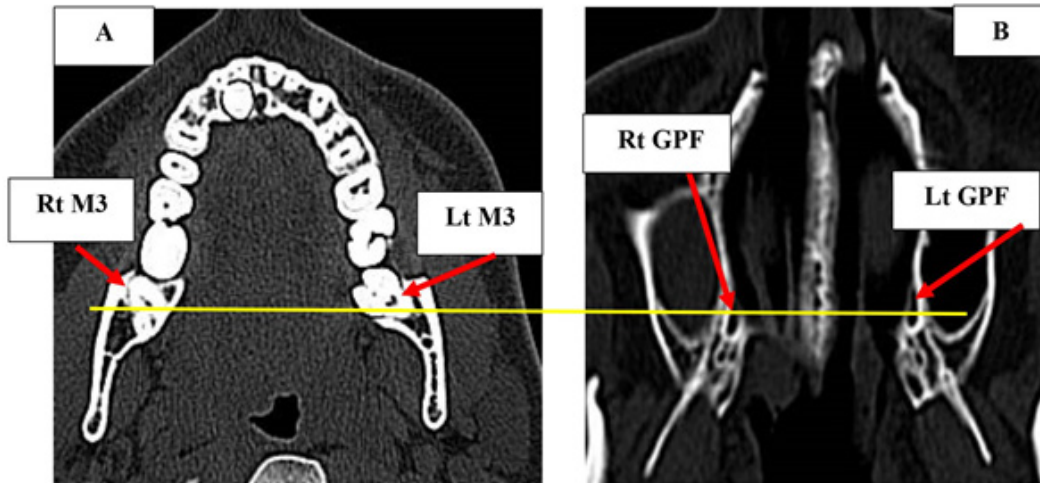


Fig. 17: Paranasal sinuses CT scan of a male patient at the region of hard palate, illustrating the right and left greater palatine foramina (GPF) (B) located opposite the right and left third maxillary molars (M3) (A).

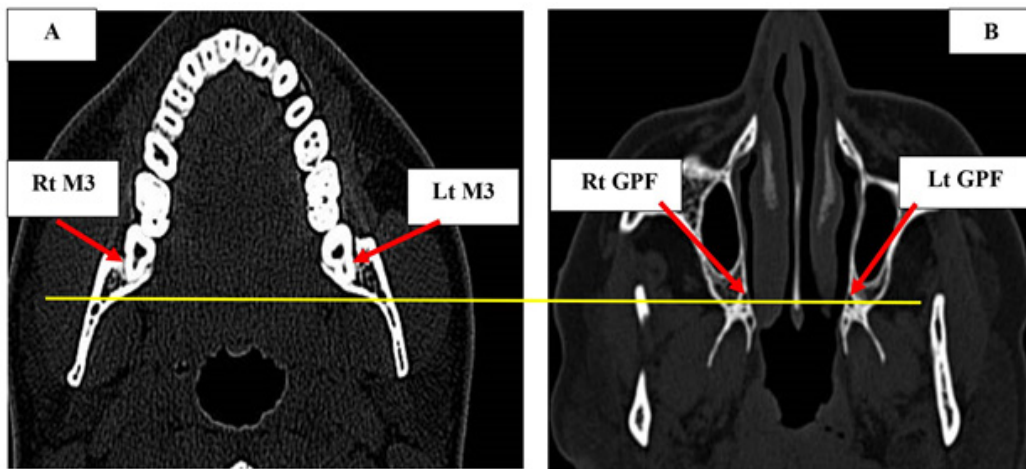


Fig. 18: A brain CT scan of a female patient at the region of hard palate, illustrating the right and left greater palatine foramina (GPF) (B) located behind the right and left third maxillary molars (M3) (A)

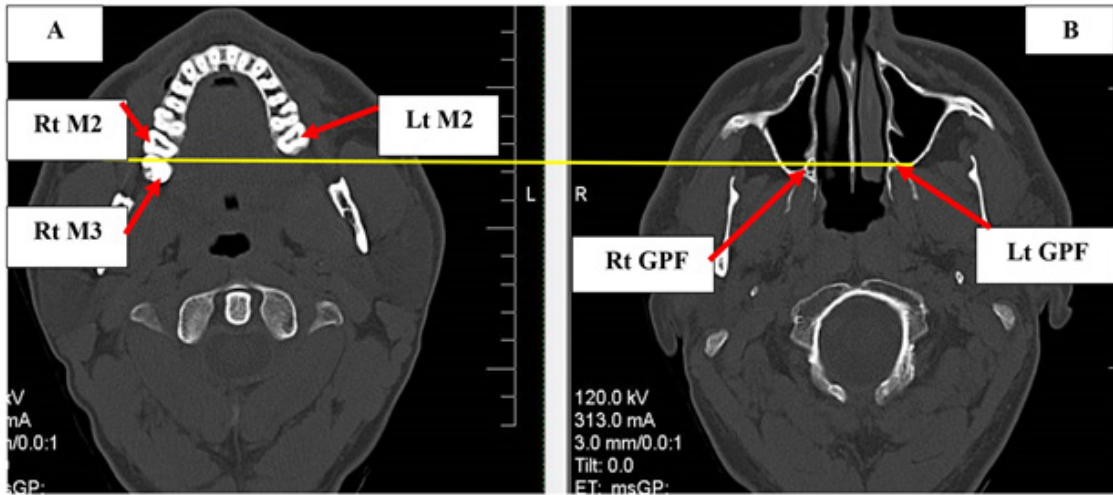


Fig. 19: Paranasal sinuses CT scan of a male patient at the region of hard palate, illustrating the right and left greater palatine foramina(GPF)(B) located between the second and third maxillary molars(M2-M3) on both sides(A)

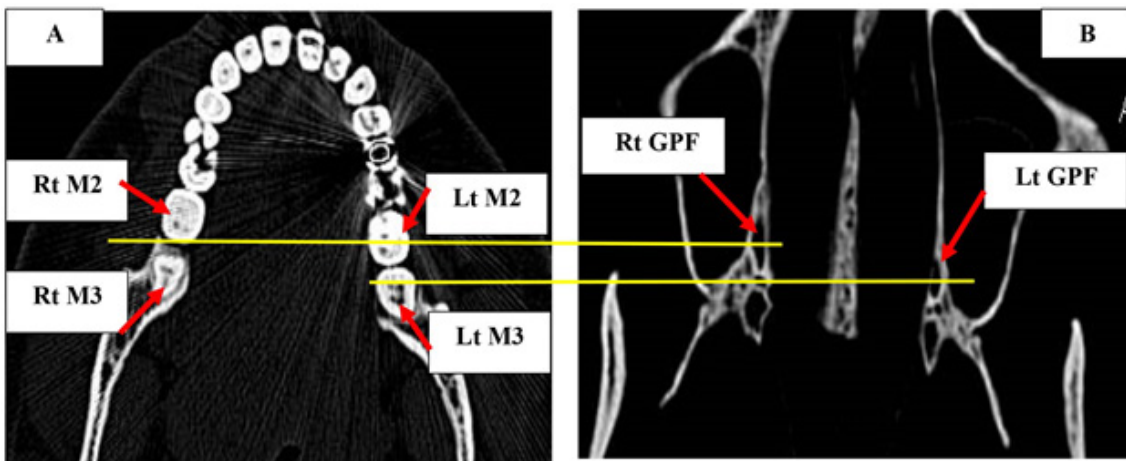


Fig. 20: A brain CT scan of a female patient at the region of hard palate, illustrating the right greater palatine foramen(GPF) (B)located between the right second and third maxillary molars(M2-M3)(A) and the left GPF(B)located opposite the left third maxillary molar(M3)(A)

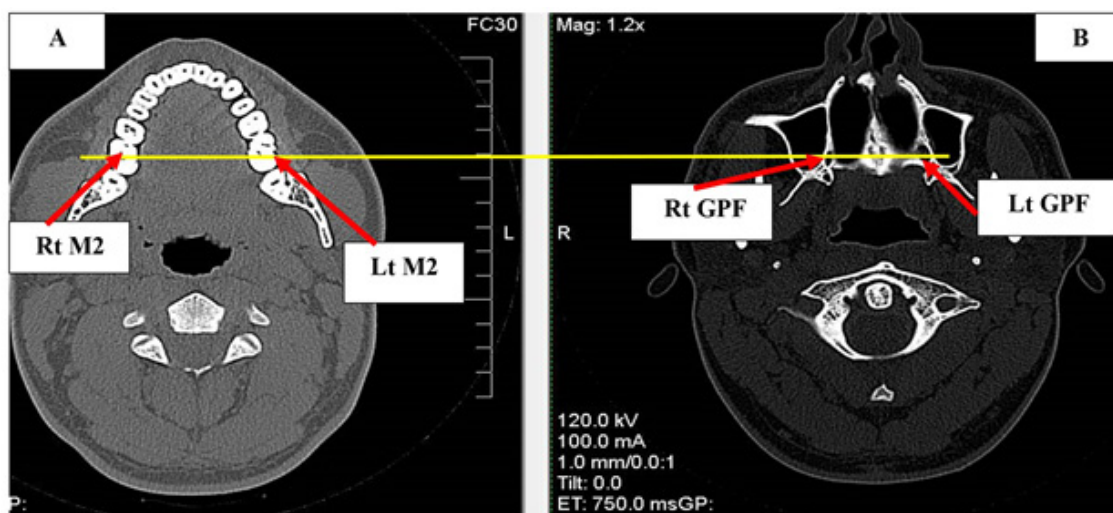
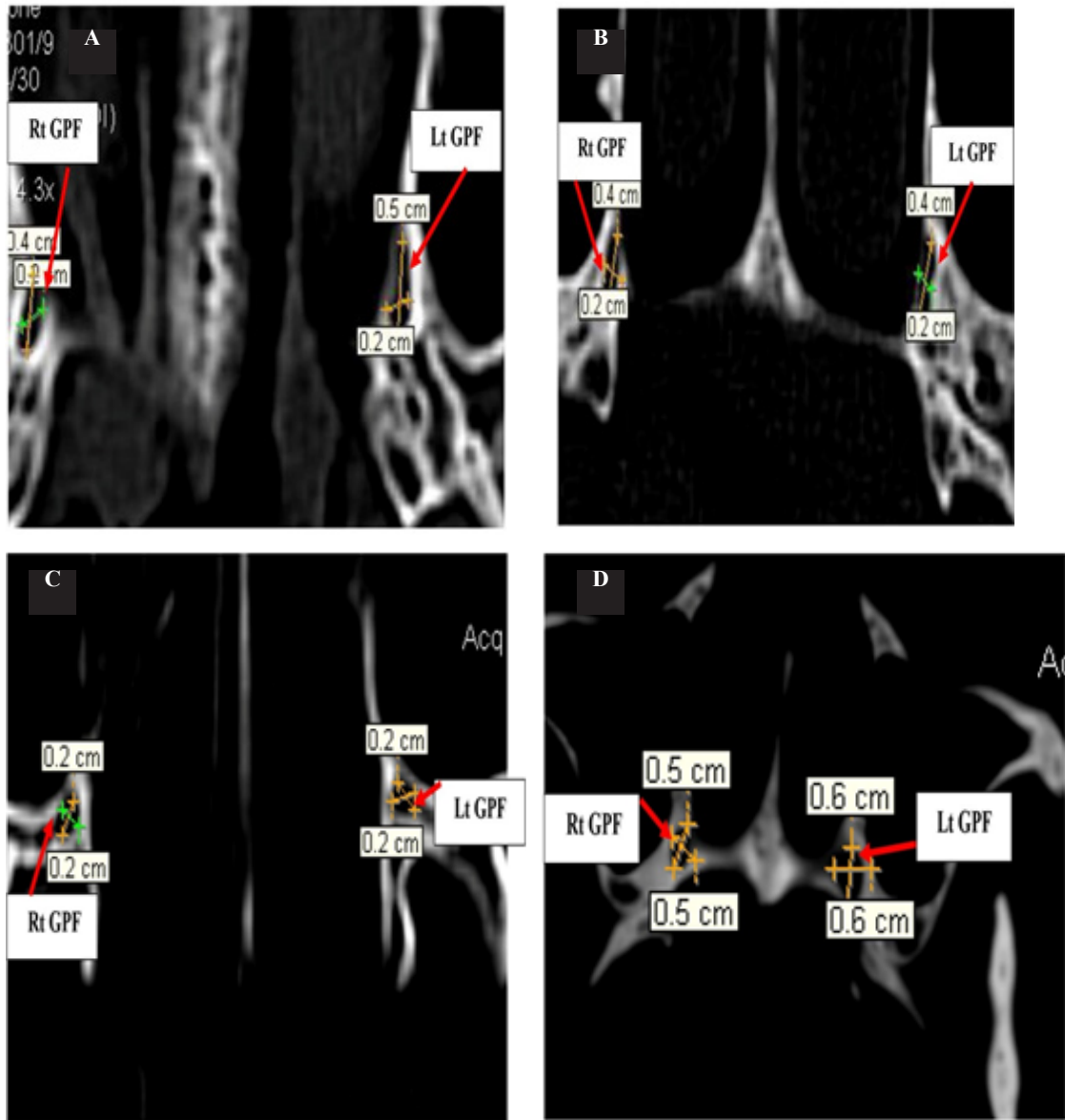


Fig. 21: Paranasal sinuses CT scan of a male patient at the region of hard palate, illustrating the right and left greater palatine foramina(GPF)(B) located opposite the right and left second maxillary molars(M2)(A)



Brain CT scan

Paranasal sinuses CT scan

A. of a male

B. of a female

C. of a female

D. of a male

Fig. 22: At the region of hard palate, illustrating the dimensions of the greater palatine foramina (GPF)

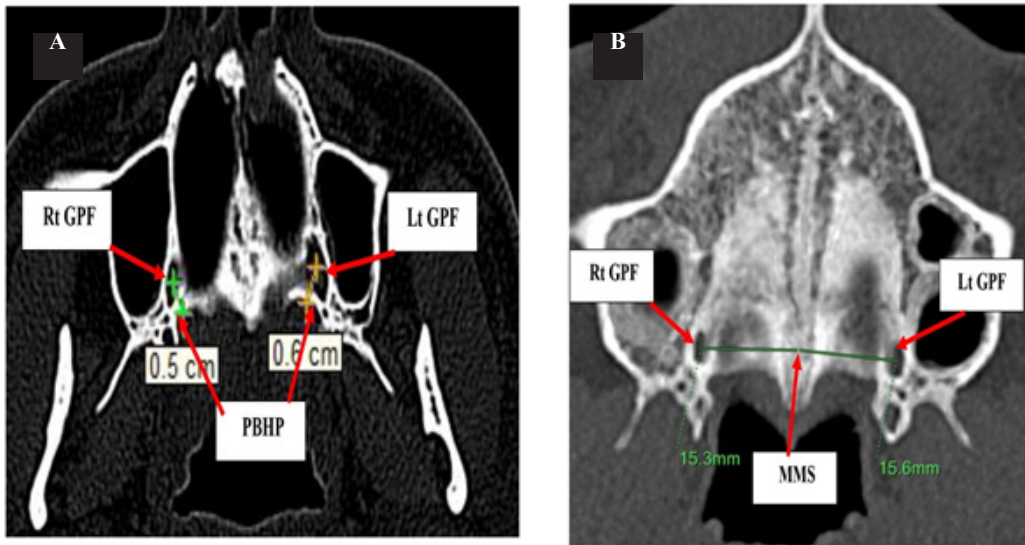


Fig. 23: A brain CT scan of a male patient at the region of hard palate, illustrating
 A. The shortest distance from the center of greater palatine foramen (GPF) to posterior border of hard palate (PBHP)
 B. The shortest perpendicular distance from the center of greater palatine foramen (GPF) to midline maxillary suture(MMS)

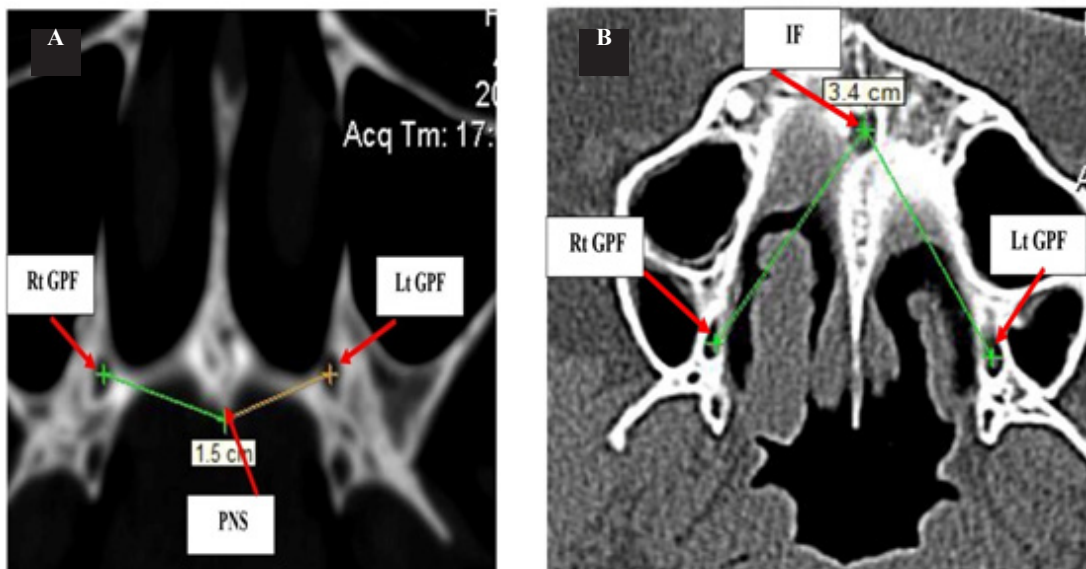
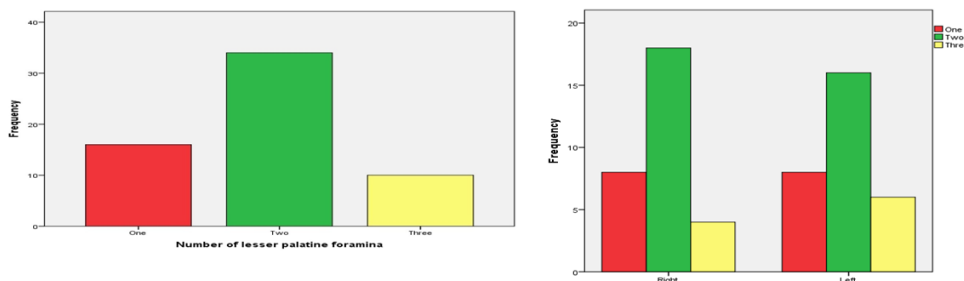
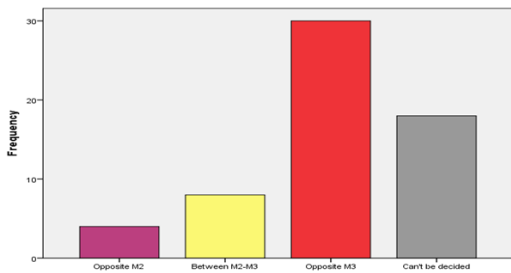


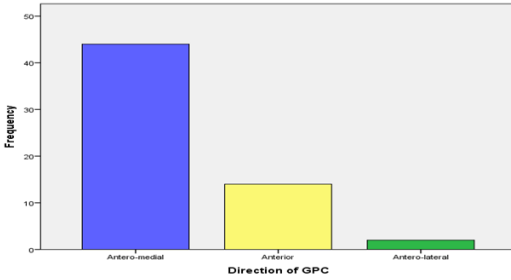
Fig. 24: Paranasal sinuses CT scan of a female patient at the region of hard palate, illustrating the distance from the center of greater palatine foramen (GPF) to posterior nasal spine (PNS), B. to incisive fossa (IF)



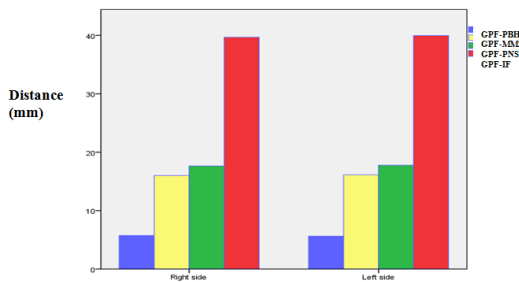
Graph 1: Bar chart of the number and frequency of lesser palatine foramen in dry skull



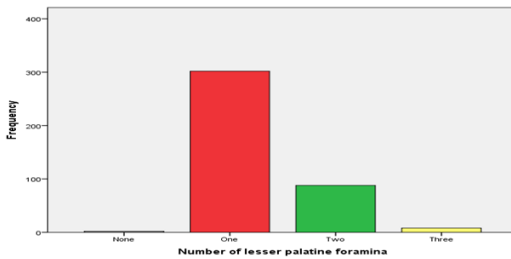
Graph 2: Bar chart of the frequency of position of the greater palatine foramen (GPF) in dry skulls



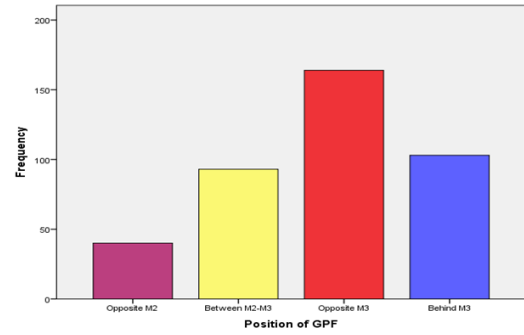
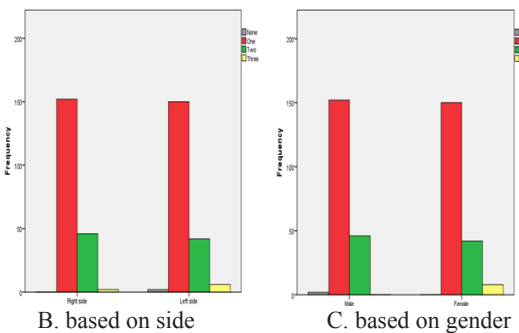
Graph 3: Bar chart of the frequency of the direction of the greater palatine canal (GPC) in dry skulls



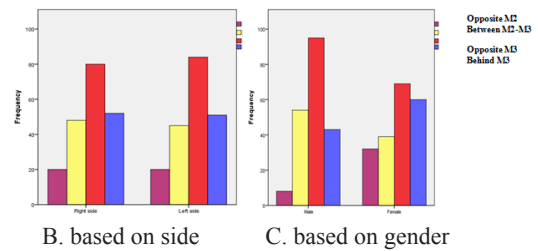
Graph 4: Bar chart of the distances taken from the center of greater palatine foramen (GPF) to surrounding anatomical landmarks in dry skulls based on side



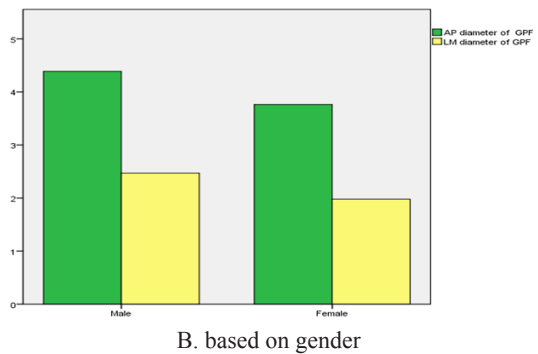
Graph 5 (A): Bar chart of the number and frequency of lesser palatine foramina in CT scans



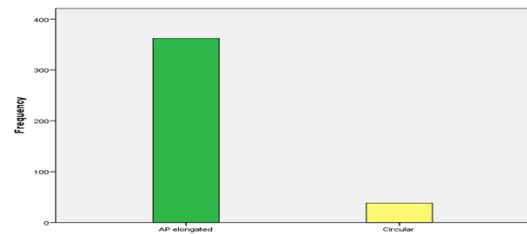
Graph 6 (A): Bar chart of the frequency of position of the greater palatine foramen (GPF) in CT scans



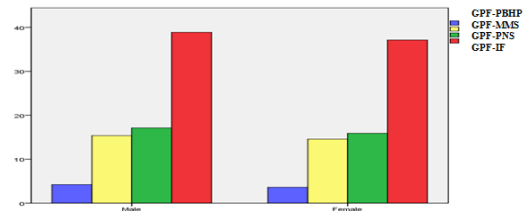
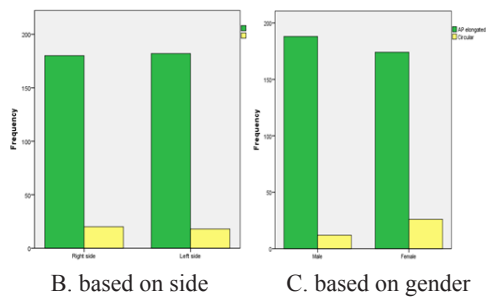
Graph 7: Bar chart of the dimensions of the greater palatine foramen (GPF) in CT scans A. based on side



B. based on gender



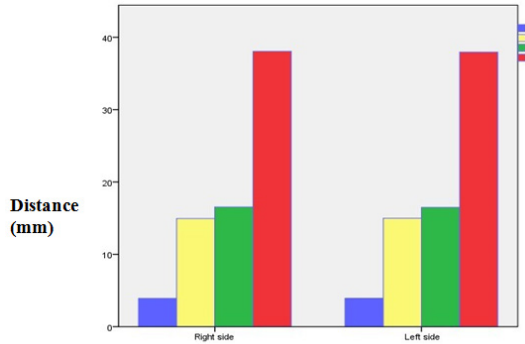
Graph (8A): Bar chart of the frequency of the shape of the greater palatine foramen (GPF) in CT scans



B. based on gender

Table 1: Number, frequency and percent of lesser palatine foramina based on side (dry skull)

Number of lesser palatine foramina	Side		Total
	Right	Left	
One	8 26.7%	8 26.7%	16 26.7%
Two	18 60.0%	16 53.3%	34 56.6%
Three	4 13.3%	6 20.0%	10 16.7%
Total	30 100.0%	30 100.0%	60 100.0%



Graph 9: Bar chart of the distances taken from the center of greater palatine foramen (GPF) to surrounding anatomical landmarks in CT scan A. based on side

Table 2: frequency and percent of the position of the GPF based on side (dry skull)

Position of GPF	Side		Total	<i>p value</i>
	Right	Left		
Opposite M3	15 50.0%	15 50.0%	30 50.0%	0.1(NS)
Opposite M2	2 6.7%	2 6.7%	4 6.7%	
Between M2-M3	4 13.3%	4 13.3%	8 13.3%	
Could not be decided	9 30.0%	9 30.0%	18 30.0%	
Total	30 100.0%	30 100.0%	60 100.0%	

p value = 0.1, statistically nonsignificant using Chi square tests
 M3: Third maxillary molar M2: Second maxillary molar

Table 3: Frequency and percent of the direction of the GPC based on side (dry skull)

Direction of GPC	Side		Total	<i>p value</i>
	Right	Left		
Antero-medial	22 73.3%	22 73.3%	44 73.3%	0.7(NS)
Anterior	7 23.3%	7 23.3%	14 23.3%	
Antero-lateral	1 3.3%	1 3.3%	2 3.3%	
Total	30 100.0%	30 100.0%	60 100.0%	

p value = 0.7, statistically nonsignificant using chi square tests

Table 4: Measurements taken from the GPF based on side (dry skull)

Measurement	Side	n	Distance (mm)	<i>p value</i>
GPF-PBHP	Right	30	5.74 ± 1.31	0.70 (NS)
	Left	30	5.61 ± 1.17	
GPF-MMS	Right	30	16.00 ± 1.30	0.70(NS)
	Left	30	16.13 ± 1.28	
GPF-PNS	Right	30	17.66 ± 1.40	0.76(NS)
	Left	30	17.77 ± 1.54	
GPF-IF	Right	30	39.70 ± 2.43	0.65 (NS)
	Left	30	39.98 ± 2.36	

*Statistically nonsignificant using independent t test

GPF-PBHP: Shortest distance from the center of greater palatine foramen to posterior border of hard palate

GPF-MMS: Shortest Perpendicular distance from the center of greater palatine to midline maxillary suture

GPF-PNS: Distance from center of greater palatine foramen to posterior nasal spine

GPF-IF: Distance from center of greater palatine foramen to center of incisive fossa

SD: Standard deviation

Table 5: Number, frequency and percent of lesser palatine foramina based on side (CT scan)

Frequency of lesser palatine foramina	Side		Total	<i>p value</i>
	Right	Left		
No foramina	0	2	2	0.5 (NS)
	0.0%	1.0%	0.5%	
One foramen	152	150	302	
	76.0%	75.0%	75.5%	
Two foramina	46	42	88	
	23.0%	21.0%	22.0%	
Three foramina	2	6	8	
	1.0%	3.0%	2.0%	
Total	200	200	400	
	100.0%	100.0%	100.0%	

p value = 0.5, statistically nonsignificant using Chi square tests

PALATINE FORAMINA ANATOMICAL VARIATIONS

Table 6: Number, frequency and percent of lesser palatine foramina based on gender (CT scan)

	Number of lesser palatine foramina				Total
	No	One	Two	Three	
Male	2 1.0%	152 76.0%	46 23.0%	0 0.0%	200 100.0%
Female	0 0.0%	150 75.0%	42 21.0%	8 4.0%	200 100.0%
Total	2 0.5%	302 75.5%	88 22.0%	8 2.0%	400 100.0%

Table 7: frequency and percent of position of the GPF based on side (CT scan)

Position of GPF	Side		Total	<i>p value</i>
	Right	Left		
Opposite M3	80 40.0%	84 42.0%	164 41.0%	<i>0.2(NS)</i>
Opposite M2	20 10.0%	20 10.0%	40 10.0%	
Between M2-M3	48 24.0%	45 22.5%	93 23.2%	
Behind M3	52 26.0%	51 25.5%	103 25.8%	
Total	200 100.0%	200 100.0%	400 100.0%	

P value = 0.2, statistically nonsignificant using Chi square tests

M3: Third maxillary molar tooth M2: Second maxillary molar tooth

Table 8: Frequency and percent of position of the GPF based on gender (CT scan)

Gender	Position of GPF				Total	<i>p value</i>
	Opposite M2	Opposite M3	Opposite M3	Behind M3		
Male	8 4.0%	54 27.0%	95 47.5%	43 21.5%	200 100.0%	<i>0.3(NS)</i>
Female	32 16.0%	39 19.5%	69 34.5%	60 30.0%	200 100.0%	
Total	40 10.0%	93 23.2%	164 41.0%	103 25.8%	400 100.0%	

p value = 0.3, statistically nonsignificant using Chi square tests

Table 9: The dimensions of the GPF based on side (CT scan)

Dimensions of GPF	Side	N	Mean ± SD	<i>p value</i>
AP dimension -GPF (mm)	Right	200	3.94 ± 1.13	0.02*
	Left	200	4.22 ± 1.21	
LM dimension -GPF (mm)	Right	200	2.17 ± 0.59	0.09
	Left	200	2.28 ± 0.74	

p value = 0.02, Statistically significant using independent t test
 AP: Anteroposterior LM: Lateral-medial

Table 10: The dimensions of the GPF based on gender (CT scan)

Dimensions of GPF	Gender	N	Mean ± SD	<i>p value</i>
AP dimension -GPF (mm)	Male	200	4.39 ± 1.20	0.000*
	Female	200	3.77 ± 1.07	
LM dimension -GPF (mm)	Male	200	2.47 ± 0.70	0.000*
	Female	200	1.98 ± 0.53	

*Statistically highly significant using independent t test

Table 11: Frequency and percent of the shape of the GPF based on side (CT scan)

Shape of GPF	Side		Total	<i>p value</i>
	Right	Left		
AP elongated	180	182	362	0.1 (NS)
	90.0%	91.0%	90.5%	
Circular	20	18	38	0.1 (NS)
	10.0%	9.0%	9.5%	
Total	200	200	400	0.1 (NS)
	100.0%	100.0%	100.0%	

p value = 0.1, statistically nonsignificant using Chi square tests

Table 12: Frequency and percent of the shape of the GPF based on gender (CT scan)

Gender	Shape of GPF		Total	<i>p value</i>
	AP elongated	Circular		
Male	188	12	200	0.02*
	94.0%	6.0%	100.0%	
Female	174	26	200	0.02*
	87.0%	13.0%	100.0%	
Total	362	38	400	0.02*
	90.5%	9.5%	100.0%	

p value = 0.02, statistically significant using Chi square tests

Table 13: Measurements taken from the GPF based on side (CT scan)

Measurement	Side	n	Distance (mm)	p value
GPF-PBHP (mm)	Right	200	3.90 ± 1.21	0.80 (NS)
	Left	200	3.93 ± 1.13	
GPF-MMS (mm)	Right	200	14.95 ± 1.30	0.75 (NS)
	Left	200	14.99 ± 1.24	
GPF-PNS (mm)	Right	200	16.55 ± 1.61	0.66 (NS)
	Left	200	16.48 ± 1.60	
GPF-IF (mm)	Right	200	38.06 ± 3.10	0.74 (NS)
	Left	200	37.96 ± 3.17	

*Statistically nonsignificant using independent t test

GPF-PBHP: Shortest distance between the center of greater palatine foramen and posterior border of hard palate

GPF-MMS: Shortest Perpendicular distance from the center of greater palatine to midline maxillary suture

GPF-PNS: Distance from center of greater palatine foramen to posterior nasal spine

GPF-IF: Distance from center of greater palatine foramen and to center of incisive fossa

SD: standard deviation

Table 14: Measurements taken from the GPF based on gender (CT scan)

Measurement	Gender	N	Distance (mm)	p value
GPF-PBHP (mm)	Male	100	4.22 ± 1.21	0.000*
	Female	100	3.61 ± 1.04	
GPF-MMS (mm)	Male	100	15.37 ± 1.21	0.000*
	Female	100	14.57 ± 1.21	
GPF-PNS (mm)	Male	100	17.13 ± 1.54	0.000*
	Female	100	15.90 ± 1.42	
GPF-IF (mm)	Male	100	38.89 ± 3.28	0.000*
	Female	100	37.13 ± 2.70	

*Statistically highly significant using independent t test

DISCUSSION

The bony palate presents the greater palatine foramen (GPF) which transmits the greater palatine neurovascular bundle. Although the palatine foramina have a great clinical significance, their exact location is vaguely described^[13]. Hence, the present study was designed to elucidate the topography of the region of the hard palate, with particular emphasis on the location of the GPF in relation to specific intraoral anatomical landmarks.

The present study was conducted on 30 dry skulls and 200 CT scans of brain and paranasal sinuses. It was found that in dry skulls the most frequent number of lesser palatine foramina (LPF) was two (56.6%) and, less common, one foramen (26.7%). This is almost analogous to the data which stated that the number of lesser palatine

foramina is usually two^[2]. However, other authors reported single LPF in 62.5% and two LPF in 30%^[17], a single LPF was found in the majority of skulls (98.53%)^[16], while others pointed out that the most frequent number of LPF was one foramen (43%), followed by two foramina in 40%^[18]. Nevertheless, literature suggests little clinical importance to matter^[8].

In dry skulls included in the present study, the least frequent number of LPF was three (16.7%). This result is close to those who reported three LPF in 15%^[18] and almost double the results of others where three LPF were recorded in 7.5%^[17]. On the other hand, multiple LPF was found in only 1.47%^[16]. Collectively, most studies conducted on dry skulls recorded a number between zero and five for LPF: (0-3)^[19]; (0-5)^[12]; (1-5)^[20] and (0-4)^[21]. High number of LPF may lead to formation of a single large LPF. Such anatomic

variation may lead to mistaking the LPF for the GPF, and thus anaesthetizing the lesser palatine nerves, causing a gag sensation in the soft palate^[8,15].

In contrast to the results of dry skulls in the present study, CT scans revealed one LPF foramen on both sides in 75.5%, two foramina in 22%, three foramina in 2% and none in 0.5% (two skulls on the left side only). It must be emphasized that the majority of studies conducted on the region of hard palate were on dry skulls^[1,5,16] and few were radiological^[11, 22-24]. None of the radiological studies investigated the number of LPF. However, the results presented in the radiological component of the present study are comparable with those conducted on dry skulls by^[11,16-18].

In the present study, although absent LPF was not encountered in dry skulls, it was met with in two in CT scans (0.5%) both on the left side. This result was similar to that reported in dry skull study which found unilateral absence of LPF in two skulls only on the left side (0.75%)^[25]. However, others reported a higher frequency: bilateral absence of LPF was encountered in two skulls (2%) and unilateral absence in twelve skulls (6%)^[26]. Absence of LPF could cause the lesser palatine nerves to exit through the GPF, and thus it becoming prone to anesthesia when blocking the greater palatine nerve^[8].

In the present study, the palatine crest was a constant finding in all dry skulls and CT scans. However, the percent of the presence of palatine crest was highly variable among previous studies. It was reported to be 67% on both sides^[15], 57.8% on the right side and 56.3% on the left^[20], 32.3% on the right side and 23.2% on the left side^[26] while listed 32.4% on the right side and 30.7% on the left^[8]. If present, palatine crest might act as a natural barrier preventing the needle from venturing into the nasopharynx^[8]. It was considered that the presence of palatine crest important in prosthetic dentistry, taking into account the thickness of the mucosa covering the GPF and the resulting minimal risk of developing pressure lesions in patients with removable dental prosthesis^[15].

In all examined dry skulls and CT scans in the present study, the presence of GPF on both sides

was also a constant finding. This is consistent with the majority of the surveyed studies^[1,5,27].

However, discrepancy in the number of GPF has previously been reported by authors who stated that "In cases where there was more than one GPF measurements were made on the larger foramen"^[20]. A single GPF was recorded in 81%, double GPF in 16% and triple GPF in 2% of the examined skulls. Multiple GPF transmit greater palatine neurovascular bundle, similar to the single GPF. The presence of multiple GPF is anticipated when the pain is not effectively blocked during anesthesia^[13]. It is an important finding as it may give rise to bleeding and hematoma during surgery^[10].

In contrast to the result of the present study on both dry skulls and CT scans, unilateral absence of the GPF has been described in 2% of cases^[13]. Those authors warned that this may weaken the potential of extracting implant tissue from the palate and reduce the chances of reconstruction. Also, complete bilateral absence of both the GPF and LPF in one skull was observed (1%)^[26].

In the present study, the GPF was most frequently located opposite M3 whether in the dry skulls (50%) or CT scans (41%). However, it is slightly difficult to rely on the results of dry skulls in this issue in particular, as the GPF couldn't be located in relation to maxillary molar teeth in 30% of the examined skulls due to obliterated alveolar ridge. Other less frequent locations were behind M3 (25.8% of CT scans), between M2-M3 (13.3% of dry skulls and 23.2% of CT scans) and opposite M2 (6.7% of dry skulls and 10% of CT scans).

The same most frequent location (opposite M3) was reported in a study on Egyptian skulls (84%)^[1]. Also, this stands in agreement with the study that found GPF most frequently located opposite M3 (74.7%), both in Europe and worldwide^[8]. Other identical studies include those in Thais^[9]; in Indians^[25]; and in Brazilians^[22].

On the other hand, a study on Chinese recorded that the most frequent location of GPF was between M2 and M3^[28], while in Thais, considered the most frequent location to be opposite M2^[29].

Despite numerous studies, there is still no agreement to whether the position of GPF is prone

to ethnic variability, this claim was supported in^[10,28,30], while this theory was refuted by^[5,15]. The cause of GPF position diversity may be due to the difference in the quality of procedures performed, as well as the way the GPF was related to maxillary molars^[8].

Regarding the direction of greater palatine canal (GPC) conducted on dry skulls only in the present study; it was found to be anteromedial in most cases (73%), anterior in 23.3% and anterolateral in 3.3%. This is in concordance with studies of^[15,16,25]. However, the canal was described as predominately anteriorly directed and not encountered with anterolateral direction^[10,28]. Furthermore, though vertical direction of the GPC has been not encountered in the present study as well as the studies of^[1,25], it was previously described in the studies of^[8,10,15,28].

Racial variation in the orientation of GPC could be used as an explanation of occasional difficulty encountered when inserting a needle into the GPF^[25]. However, it was warned that estimating the direction of GPC has been proven inaccurate, as different authors use different estimation methods and introducing needles into GPF is considered a very rough one^[8]. The latter authors stressed that the only sure way to determine the direction of the GPC is to base on horizontal and sagittal CT scans. Additionally, it was reported that the frequency of anatomical obstruction of the needle in the GPC increases with age^[31].

The clinical importance of such demarcation lies in the fact that the direction of GPC helps in proper introduction of the needle into the GPF and gives an idea for the path to be traced up into the GPC^[26]. Furthermore, the occurrence of an anterolaterally directed GPC is of clinical significance, as it is difficult to negotiate such canal with a needle^[14]. It was suggested that the difficulty in negotiating the canal may be due to its tortuosity, as seen in 5% of the population, or due to exostosis on the medial pterygoid plate that comprises the posterior border of the canal^[32].

In the present study, the dimensions of the GPF were estimated only radiologically; in dry skulls, the GPF is too narrow to allow negotiation with the double tipped compass. The mean AP diameter was 3.94 ± 1.13 mm on the right side and 4.22 ± 1.21 mm on the left, while the mean LM diameter was 2.17 ± 0.59 mm on the right

side and 2.28 ± 0.74 mm on the left. The GPF was described as AP elongated in 90.5% and circular in 9.5%. These results are almost close to those of^[5,8].

However, a study was conducted on Egyptian population and measured the mean AP as 4.86 ± 0.9 mm on the right side and 4.78 ± 1.01 mm on the left. The mean LM diameter was 3.02 ± 0.7 mm on the right side and 3.01 ± 0.9 mm on the left side^[1]. The discrepancy between the present study and that of the latter study could be attributed to the fact that measurements in the present study were obtained radiologically different because the other study was performed manually on dry skulls. Moreover, the GPF was described as frequently oval (71%), rounded in 22%, lancet and slit shaped in the remaining; the latter authors did not specify the method of determining the shape^[1].

The present study elucidates that the difference in locating the GPF in relation to maxillary molars could be due to lack of a unified methodology rather than ethnic variation. The same opinion has been adopted by a study which regarded it very important to consider the shape of the GPF when referencing it to the maxillary molars, and to measure the relation of the center of GPF to maxillary molars, rather than to one of its borders^[8].

In this work, it was attempted to locate the GPF in relation to specific surrounding anatomical landmark such as posterior border of hard palate (PBHP), midline maxillary suture (MMS), posterior nasal spine (PNS) and incisive fossa (IF). In dry skulls, the mean distance from the center of GPF to PBHP was 5.74 ± 1.30 mm on the right side and 5.61 ± 1.17 mm on the left. This is close to results of^[8,12]. An Egyptian study on dry skulls measured the GPF-PBHP distance as 4.39 ± 1.73 mm on the right side and 4.53 ± 1.23 mm on the left. However, the measurements were taken from the posterior edge of GPF to the point of maximum concavity on PBHP, while in the present study it was taken from the center of GPF to the shortest distance on the posterior border of hard palate^[1].

On the other hand, the GPF-PBHP distance was measured as 3.5 ± 0.2 mm on both sides^[14] and as 3.4 ± 1.2 mm on the right side and 3.5 ± 1.1 mm on the left^[33].

The variability in GPF-PBHP distance could be attributed to the sutural growth between maxilla and palatine bone^[31]. The difference in GPF-PBHP distance can be explained by growth at the level of transverse palatine suture and by the fact that the palate length increases anteriorly from this suture after lateral teeth eruption^[5]. At the same time, the growth is significantly reduced posteriorly from this line. Another explanation lies in the fact that some authors refer the GPF to the lateral most aspect of PBHP^[15], while others, to the greatest concavity of the PBHP^[14].

In the present study on CT scans, the GPF-PBHP distance was 3.9 ± 1.21 mm on the right side and 3.93 ± 1.13 mm on the left. This is consistent with a study where GPF-PBHP distance was recorded as 3.63 ± 1.91 mm on the right side and 3.94 ± 1.97 mm on the left^[34].

The difference in the present study between GPF-PBHP distance on dry skulls and CT scans could be attributed to the accuracy of procedure performed. A double tipped compass was used on dry skulls and this in particular was difficult to be negotiated, being the shortest of all the estimated distances. On the other hand, in CT scans data were obtained using the measuring tool of the e-film program with minimal human error.

The distance between GPF-PBHP holds its importance in successful localization of GPF and prevention of accidental injury to nearby lesser palatine nerves and soft palate. Moreover, this dimension helps in localization of GPF in these cases where the third maxillary molar failed to erupt or is damaged due to any reason^[35].

In the present study on dry skulls, the mean distance from the center of GPF to MMS was 16 ± 1.30 mm on the right side and 16.13 ± 1.28 mm on the left, similar to results of^[9,36,37] but far from results of which the GPF-MMS distance was estimated as 14.82 ± 1.34 mm on the right side and 14.79 ± 1.57 mm on the left^[1,10].

In the present work, the mean distance from the center of GPF to PNS was 17.66 ± 1.40 mm on the right side and 17.77 ± 1.54 mm on the left. This measurement was not previously addressed whether in dry bone or radiological studies, apart from that of a study where it was measured as 17 ± 1.5 mm on both sides^[8]. The latter authors emphasized that its importance

lies in locating the GPF in edentulous patients. Nevertheless, the posterior margin of hard palate, though clinically visible due to its narrow mucous membrane band of lighter color, is not recommended as a reference point, being not practical clinically^[5].

In the present study on dry skulls, the mean distance from the center of GPF to the center of IF was 39.70 ± 2.43 on the right side and 39.98 ± 2.36 mm on the left, close to results provided by^[38], but not to those of other study in which GPF-IF distance was measured as 37.09 ± 3.3 mm on the right side and 37.08 ± 3.7 mm on the left^[1].

In the present study on dry skulls, the mean distance from the center GPF to the center of opposite GPF was 30.38 ± 2.36 mm. This measurement also, was not previously negotiated whether in dry bone or radiological studies, except in that of a study in which its mean value was calculated as 29.1 ± 2.6 mm with no obvious clinical importance^[8].

Comparing the results of the present study on dry skulls with those obtained also in Egyptian population, their values were statistically non-significantly smaller¹. This difference could be attributed to the methodology of measurement; the latter authors adopted the methodology and measured GPF-MMS distance from the medial edge of GPF to shortest perpendicular distance to MMS and measured GPF-IF distance from anterior edge of GPF to posterior border of IF^[10]. On the other hand, all measurements in the present study were taken from the center of GPF and the center of IF. Taking the measurements from the margins of GPF was considered questionable due to variations in the shape of the foramen^[33].

The importance of GPF-IF distance was emphasized in determining the site of GPF in conditions with absent maxillary molar teeth and patients with midline palatal defects creating difficulty in locating MMS^[35].

Linear measurements performed on CT scans in the present study, showed the mean distance from the center of GPF to MMS as 14.95 ± 1.3 mm on the right side and 14.99 ± 1.24 on the left. These values were close to radiological results in which the GPF-MMS distance was estimated as 15.2 ± 1.45 mm^[22]. In the present study the mean distance from the center of GPF to PNS was

16.55 ± 1.61 mm on the right side and 16.48 ± 1.6 mm on the left while the distance from the center of GPF to the center of IF was 38.06 ± 3.10 on the right side and 37.96 ± 3.17 on the left. These figures are disparate from the radiological results which estimated the GPF-MMS distance as 34 ± 3 mm on the right side and 34.3 ± 3.1 on the left, though the same methodology was applied in both studies^[8].

Comparing the results in both dry skulls and CT scans in the present study, showed that no statistically significant side difference exists in the linear measurements from the center of GPF to surrounding anatomical landmarks. This goes with studies that agreed that linear measurements of the GPF with respect to the surrounding anatomical landmarks did not vary significantly between the sides, demonstrating a remarkable bilateral symmetry^[1,9,15,16,25]. On the contrary, a statistically significant difference in linear measurements between sides was reported^[8,38]. The latter authors attributed this difference to palatal development, which depends on the function of several ossification centers^[31].

In the present study a statistically significant side difference was found in the dimensions of GPF. Previous radiological studies provided no data regarding this point^[8,22,23]. Although a statistically significant difference between the dimensions of GPF on both sides was not recognized in the study on dry skulls, radiological data should be considered more accurate in this respect^[1].

In the present study, a statistically highly significant difference in linear measurements from the center of GPF to surrounding anatomical landmarks as well as the dimensions of GPF existed between males and females. This is similar to results of^[1,8,9,38]. Male skulls are generally larger and more massive the female ones^[38]. Moreover, adult human skulls are composed of a set of bones that are extremely rich in information concerning sexual dimorphism, which can be assessed both qualitatively and quantitatively^[39].

Although a statistically significant difference between males and females was observed regarding the distance from GPF to IF, no statistically significant difference existed regarding the distance between right and left GPF^[39,40].

CONFLICT OF INTERESTS

There are no conflicts of interest.

REFERENCES

1. Shalaby, S A, Eid, E M, Sarg, N A, Sewilam, A M. Morphometric analysis of hard palate in Egyptian skulls. *Benha Medical Journal*, 2015.32(1): 59-72.
2. Standring, S, Black, S, Gleeson, M. *et al.* External skull, In: *Gray's Anatomy: The Anatomical Basis of Clinical Practice*, 41st edition, Michael Gleeson, ed, Elsevier Health Sciences, London, 2016.UK. Chapter 27, p: 416-428.
3. Costa, H, Zenha, H, Sequeira, H, Coelho, G, Gomes, N, Pinto, C Andresen, C. Microsurgical reconstruction of the maxilla: Algorithm and concepts. *Journal of Plastic, Reconstructive & Aesthetic Surgery*, 2015.68(5): e89-e104.
4. Yu, S K, Lee, M H, Park, B S, Jeon, Y H, Chung, Y Y, Kim, H J. Topographical relationship of the greater palatine artery and the palatal spine. Significance for periodontal surgery. *Journal of Clinical Periodontology*, 2014. 41(9): 908-913.
5. Nimigean, V, Nimigean, V R, Buțincu, L A, Sălăvăstru, DI, Podoleanu, L. Anatomical and clinical considerations regarding the greater palatine foramen. *Rom J MorpholEmbryol*, 2013.54(3 Suppl): 779-783.
6. Newman MG, Takei HH, Klokkevold PR, Carranza FA. *Carranza's Clinical Periodontology*, 10thedn. Saunders/Elsevier, Philadelphia/Amsterdam, 2007.pp: 1008–1014.
7. Moore, KL, Dalley, AF, Agur, AM. *The Palate*. In: *Clinically oriented anatomy, Head*, 7th edition. Moore, K.L., Dalley, A.F. and Agur, A.M. eds. Lippincott Williams and Wilkins, Philadelphia, USA, 2013.pp: 935-937.
8. Tomaszewska, I M, Kmiotek, E K, Pena, I Z, Średniawa, M, Czyżowska, K, Chrzan, R, Walocha, J A. Computed tomography

- morphometric analysis of the greater palatine canal: A study of 1,500 head CT scans and a systematic review of literature. *Anatomical Science International*, 2015. 90(4): 287-297
9. Methathrathip D, Apinhasmit W, Chompoopong S, *et al.* Anatomy of greater palatine foramen and canal and pterygopalatine fossa in Thais: considerations for maxillary nerve block. *Surg.Radiol.Anat.*, 2005.27: 511–516.
 10. Chrcanovic, B R, Custódio, A L. Anatomical variations in the position of the greater palatine foramen. *Journal of Oral Science*, 2010.52(1):109-113.
 11. Hwang, S H, Seo, J H, Joo, Y H, Kim, B G, Cho, J H, Kang, J M. An anatomic study using three-dimensional reconstruction for pterygopalatine fossa infiltration via the greater palatine canal. *Clinical Anatomy*, 2011.24(5): 576-582.
 12. Osunwoke, E A, Amah-Tariah, F S, Bob-Manuel, I F, Nwankoala, Q K. A study of the palatine foramen in dry human skulls in South-South Nigeria. *Scientia Africana*, 2011.10(1):98-101.
 13. Cagimni, P, Govsa, F, Ozer, M A, Kazak, Z. Computerized analysis of the greater palatine foramen to gain the palatine neurovascular bundle during palatal surgery. *Surgical and Radiologic Anatomy: SRA*, 2017.39(2): 177-184.
 14. Ajmani, M L. Anatomical variation in position of the greater palatine foramen in the adult human skull. *Journal of Anatomy*, 1994.184(3): 635-637.
 15. Jaffar, A A, Hamadah, H J. An analysis of the position of the greater palatine foramen. *J Basic Med Sci*, 2003.3(1): 24-32.
 16. Ilayperuma, I, Nanayakkara, G, Palahepitiya, N. Morphometric Evaluation of the Greater Palatine Foramen in Adult Sri Lankan Skulls. *International Journal of Morphology*, 2014.32(4): 1418-1422.
 17. D'Souza, A S, Mamatha, H, Jyothi, N. Morphometric analysis of hard palate in south Indian skulls. *Biomed Res*, 2012. 23: 173-175.
 18. Sushobhana, S R, Singh, S, Jigyasa Passey, R S, Sinh, A P. Anatomical Study and Clinical Considerations of Greater Palatine Foramen in Adult Human Skulls of North Indian Population. *International Journal of Anatomy, Radiology and Surgery*, 2015.4(4): 41-46.
 19. Kumar, A, Sharma, A, Singh, P. Assessment of the relative location of greater palatine foramen in adult Indian skulls: consideration for maxillary nerve block. *Eur J Anat*, 2011.15(3): 150-154.
 20. Piagkou, M, Xanthos, T, Anagnostopoulou, S, Demesticha, T, Kotsiomitris, E, Piagkos, G, Johnson, E O. Anatomical variation and morphology in the position of the palatine foramina in adult human skulls from Greece. *Journal of Cranio-Maxillofacial Surgery*, 2012.40(7): e206-e210.
 21. Jotania, B, Patel, S V, Patel, S M, Patel, P, Patel, S., Patel, K. Morphometric analysis of hard palate. *Int J Res Med*, 2013. 2(2): 72-75.
 22. Renata, C, Ikuta, S, Cardoso, C L, Ferreira-júnior, O, Roberto, J, Lauris, P, Rubira-bullen, F. Position of the greater palatine foramen: an anatomical study through cone beam computed tomography images. *Surgical and Radiologic Anatomy*, 2013.35(9): 837.
 23. Asha, ML, Arun Kumar, G, Sattigeri Anupama, V, Raja Jigna, V, Diksha, M. Cone beam computed tomographic analysis of anatomical variations of greater palatine canal and foramen in relation to gender in South Indian population. *Oral Health Dent Manag*, 2015.14: 384-390.
 24. Aoun, G, Nasseh, I, Sokhn, S. Radio-anatomical study of the greater palatine canal and the pterygopalatine fossa in a Lebanese population: a consideration for maxillary nerve block. *Journal of Clinical Imaging Science*, 2016.6:35
 25. Saralaya, V, Nayak, S R. The relative position of the greater palatine foramen in dry Indian skulls. *Singapore Medical Journal*, 2007.48(12): 1143-1146.

26. Sharma, N A, Garud, R S. Greater palatine foramen--key to successful hemimaxillary anaesthesia: a morphometric study and report of a rare aberration. *Singapore Medical Journal*, 2013.54(3):152-159.
27. Ikuta, C R, Cardoso, C L, Ferreira-Júnior, O., Lauris, J R, Souza, P H, Rubira-Bullen, I R. Position of the greater palatine foramen: an anatomical study through cone beam computed tomography images. *Surgical and Radiologic Anatomy*, 2013.35(9): 837-842.
28. Wang, T M, Kuo, K J, Shih, C., Ho, L L, Liu, J C. Assessment of the relative locations of the greater palatine foramen in adult Chinese skulls. *Cells Tissues Organs*, 1988. 132(3): 182-186.
29. Klosek, S K, Rungruang, T. Anatomical study of the greater palatine artery and related structures of the palatal vault: considerations for palate as the subepithelial connective tissue graft donor site. *Surg. and Radiol. Anat.*, 2009. 31(4): 245-250.
30. Cutright, B, Quillopa, N, Schubert, W. An anthropometric analysis of the key foramina for maxillofacial surgery. *Journal of Oral and Maxillofacial Surgery*, 2003.61(3): 354-357.
31. Slavkin, H C, Canter, M R, Canter, S R. An anatomic study of the pterygomaxillary region in the craniums of infants and children. *Oral Surgery, Oral Medicine, Oral Pathology*, 1966.21(2): 225-235.
32. Hawkins, J M, and Isen, D. Maxillary nerve block: the pterygopalatine canal approach. *Journal of the California Dental Association*, 1998. 26(9): 658-664.
33. Lopes PT, Santos AM, Pereira GA *et al.* Morphometric analysis of the greater palatine foramen in dry Southern Brazilian adult skulls. *Int J Morphol*, 2011.29: 420-424
34. Rapado-González, O, Suárez-Quintanilla, J A, Otero-Cepeda, X L, Fernández-Alonso, A, Suárez-Cunqueiro, M M. Morphometric study of the greater palatine canal: cone-beam computed tomography. *Surgical and Radiologic Anatomy*, 2015.37(10): 1217-1224.
35. Sharma, N, Varshney, R, Ray, S. Anatomic and anaesthetic considerations of greater palatine nerve block in Indian population. *Saudi Journal of Medicine and Medical Sciences*, 2014.2(3): 197-201.
36. Urbano, E S, Melo, K A, Costa, S T. Morphologic study of the greater palatine canal. *J Morphol Sci*, 2010.27, 102-4.
37. Dave, M R, Yagain, V K, Anadkat, S. A study of the anatomical variations in the position of the greater palatine foramen in adult human skulls and its clinical significance. *Int J Morphol*, 2013. 31: 578-583.
38. Teixeira, C, Souza, V, Marques, C, Silva Junior, W., Pereira, K. Topography of the greater palatine foramen in macerated skulls. *J Morphol Sci*, 2010.27: 88-92.
39. Nascimento, L, Lima, C, de Oliveira, O F, Sassi, C, Picapedra, A, Júnior, L F, Júnior, E D. Sex determination by linear measurements of palatal bones and skull base. *Journal of Forensic Odonto-Stomatology*, 2012.30(1): 37-44.
40. Moreira, R S, Sgrott, E A, Stuker, H, Alonso, L G, Smith, R L. Palatal asymmetry during development: an anatomical study. *Clinical Anatomy*, 2008.21(5): 398-404.

دراسة الاختلافات التشريحية في عدد ومكان الأثقاب الحنكية بين المصريين

دراسة بالعظم الجاف والاشعة

إ.د / محمد عماد الدين ابراهيم محمد

د/ حنان نبيه جاد الله د/ احمد سيد عوض هدير ماهر احمد تهاى

قسم التشريح و علم الاجنه وقسم الاشعة

ملخص البحث

يمثل الثقب الحنكي الأكبر أهم منطقة في باطن الحلق كونه الأكثر والأدق تمثيلاً في القشرة المخية الحسية الحركية بالمقارنة بباقي العناصر التشريحية في هذه المنطقة.

اجريت هذه الدراسة على ٣٠ جمجمة جافة غير معلومة الجنس و ٢٠٠ أشعة مقطعية على المخ و الجيوب الأنفية (١٠٠ ذكر وبالغ و ١٠٠ انثى بالغة). تم تصميم هذه الدراسة لتحديد مكان وجود الثقب الحنكي الأكبر بالنسبة للمعالم التشريحية المحيطة لما له من أهمية أساسية لكل من أطباء الفم والأسنان و جراحي الوجه و الفكين.

كان عدد للثقوب الحنكية الصغرى الأكثر شيوعاً في الجمجم الجافة هو اثنين بنسبة ٥٦,٧٪, أقل شيوعاً كان واحد بنسبة ٢٦,٧٪, ثلاثة بنسبة ١٦,٧٪ دون وجود فرق ذو دلالة إحصائية في عدد الثقوب بين الجانبين. أما في الأشعات المقطعية فكان أكثر الأعداد شيوعاً للثقوب الحنكية الصغرى هو ثقب واحد بنسبة ٧٥,٥٪, أقل شيوعاً كان اثنين بنسبة ٢٢٪, ثلاثة بنسبة ٢٪, كان غير موجود في ٠,٥٪ وكما في الجمجم الجافة لم يكن هناك فرق ذو دلالة إحصائية في عدد الثقوب بين الجانبين.

بالنسبة للعلاقة بين مكان الثقب الحنكي الأكبر و أضرار الفك العلوي, وجد في هذه الدراسة ان أكثر تواجد شيوها هو في مقابلة الضرس الثالث في ٥٠٪ من الجمجم الجافة, ٤١٪ من الأشعات المقطعية, أقل شيوعاً بين الضرس الثاني والثالث في ١٣,٣٪ من الجمجم الجافة, ٢٣,٣٪ من الأشعات المقطعية, خلف الضرس الثالث في ٢٥,٨٪ من الأشعات المقطعية, في مقابلة الضرس الثاني في ٦,٧٪ من الجمجم الجافة, ١٠٪ من الأشعات المقطعية.

تم تحديد اتجاه القناة الحنكية الكبرى على الجمجم الجافة وقد تبين أنه أمامي أنثى في ٧٣٪, أمامي في ٢٣,٣٪, أمامي وحشي في ٣,٣٪, و قد وجد نفس الاتجاه على الجانبين.

تم قياس أبعاد الثقب الحنكي الأكبر في الأشعة, كان متوسط القطر الأمامي الخلفي على الجانب الأيمن $3,94 \pm 1,13$ مم, على الجانب الأيسر $4,22 \pm 1,21$ مم, و متوسط القطر الجانبي الوسطي على الجانب الأيمن $2,17 \pm 0,59$ مم, على الجانب الأيسر $2,28 \pm 0,74$ مم. و قد وجد ان الثقب الحنكي الأكبر ممتد من الأمام للخلف في ٩٠,٥٪, مستدير في ٩,٥٪ من الأشعات المقطعية التي تم فحصها و بمقارنة الجانب الأيمن والأيسر وجد ان هناك فرق ذو دلالة إحصائية في القياسات.

تم حساب القياسات الخطية من مركز الثقب الحنكي الأكبر الى المعالم التشريحية المحيطة في كل من الجمجم الجافة و الأشعات المقطعية. بالنسبة للجمجم الجافة كان متوسط المسافة من مركز الثقب الحنكي الأكبر حتى الحد الخلفي للحنك الصلب $5,74 \pm 1,31$ مم على الجانب الأيمن, $5,61 \pm 1,17$ مم على الجانب الأيسر, و متوسط المسافة من مركز الثقب الحنكي الأكبر حتى خط الوسط في الفك العلوي $16 \pm 1,30$ مم على الجانب الأيمن, $16,13 \pm 1,28$ مم على الجانب الأيسر, و متوسط المسافة من مركز الثقب الحنكي الأكبر حتى الشوكة الخلفية للألف $17,66 \pm 1,40$ مم على الجانب الأيمن, $17,77 \pm 1,54$ مم على الجانب الأيسر, و متوسط المسافة من مركز الثقب الحنكي الأكبر الى مركز الحفرة القاطعة $39,70 \pm 2,43$ مم على الجانب الأيمن, $39,98 \pm 2,36$ مم على الجانب الأيسر, و متوسط المسافة من مركز الثقب الحنكي الأكبر الى مركز الثقب الحنكي المقابل $31,81 \pm 2,58$ مم.

في الأشعات المقطعية كان متوسط المسافة من مركز الثقب الحنكي الأكبر حتى الحد الخلفي للحنك الصلب $3,9 \pm 1,21$ مم على الجانب الأيمن, $3,93 \pm 1,13$ مم على الجانب الأيسر, و متوسط المسافة من مركز الثقب الحنكي الأكبر حتى خط الوسط في الفك العلوي $14,95 \pm 1,3$ مم على الجانب الأيمن, $14,99 \pm 1,24$ مم على الجانب الأيسر, و متوسط المسافة من مركز الثقب الحنكي الأكبر حتى الشوكة الخلفية للألف $16,55 \pm 1,61$ مم على الجانب الأيمن, $16,48 \pm 1,6$ مم على الجانب الأيسر, و متوسط المسافة من مركز الثقب الحنكي الأكبر الى مركز الحفرة القاطعة $38,06 \pm 3,10$ مم على الجانب الأيمن, $37,96 \pm 3,17$ مم على الجانب الأيسر, و متوسط المسافة من مركز الثقب الحنكي الأكبر على احد الجانبين الى مركز الثقب الحنكي المقابل $31,22 \pm 2,30$ مم.

بالنسبة للقياسات الخطية لم يكن هناك فرق ذو دلالة إحصائية بين الجانب الأيمن والأيسر, بينما كان هناك فرق ذو دلالة إحصائية في القياسات بين الأنثى والذكور.